IZDEVNIECĪBA
BALTIJA
PUBLISHING

GLOBAL TRENDS AND PROSPECTS OF SOCIO-ECONOMIC DEVELOPMENT OF UKRAINE

Scientific monograph

Riga, Latvia
2022

UDK 33(477)(08)
Gl543

Title: Global trends and prospects of socio-economic development of Ukraine

Subtitle: Scientific monograph

Scientific editor and project director: Anita Jankovska

Authors: Yuliia Aleskerova, Volodimir Todosiichuk, Valeriia Vovk, Anastasiia Krasnoselska, Lyudmila Volontyr, Nadiia Hryshchuk, Svitlana Kovalchuk, Olena Martseniuk, Lyudmila Novitska, Oksana Ruda, Dina Tokarchuk, Oleksiy Tokarchuk, Inna Tomashuk, Ivan Tomashuk, Olena Tomchuk, Olha Khaietska, Oleksandr Shevchuk, Svitlana Kiporenko, Oleksandr Shevchuk, Olena Shevchuk, Viktor Dzis, Olena Dyachynska, Viktor Dubchak, Elvira Manzhos, Svitlana Bogatchuk, Yurii Boiko, Zorislav Makarov, Diana Bohatyrchuk, Kostiantin Levchuk, Elena Levchuk, Natalia Havryliuk

Publisher: Publishing House "Baltija Publishing", Riga, Latvia

Available from: http://www.baltijapublishing.lv/omp/index.php/bp/catalog/book/205

Year of issue: 2022

Global trends and prospects of socio-economic development of Ukraine: Scientific monograph. Riga, Latvia: Baltija Publishing, 2022. 688 p.

ISBN: 978-9934-26-193-0

DOI: https://doi.org/10.30525/978-9934-26-193-0

The scientific monograph presents the global trends and prospects of socio-economic development of Ukraine. General questions of economics and enterprise management, regional economics, marketing, modern management, general pedagogy and history of pedagogy, theory and methods of vocational education, general questions of historical sciences, and so on are considered. The publication is intended for scientists, educators, graduate and undergraduate students, as well as a general audience.

Table of Contents

CHAPTER «ECONOMIC SCIENCES»

CHAPTER «HISTORICAL SCIENCES»

CHAPTER «PEDAGOGICAL SCIENCES»

CHAPTER «TECHNICAL SCIENCES»

VISCOSITY AND THERMAL CONDUCTIVITY OF RUBIDIUM AND CESIUM IN THE GAS PHASE

Viktor Dzis[1]
Olena Dyachynska[2]

DOI: https://doi.org/10.30525/978-9934-26-193-0-16

Abstract. An experimental installation has been developed to study the viscosity of alkali metal vapor in a wide range of high (up to 2000 K) temperatures, which implements the method from a viscometer with an annular channel. The design of the viscometer of the measuring cell makes it possible to directly measure the temperature of the working element of the viscometer. This provides an accurate determination of the temperature of the investigated alkali metal vapor in the working gap.

The original method of stabilization of the steam generator operation mode was applied, which allowed to ensure the stationary flow of the investigated alkali metal vapor in the working element of the viscometer. Distinctive features of the created installation are high stability of modes of its work and considerable resource.

An experimental study of the viscosity of rubidium and cesium in the gas phase was carried out by the method of a viscometer with an annular channel at the following values of the state parameters:

for cesium T = 900 ... 1770 K, P = 12 ... 135 kPa;

for rubidium T = 990 ... 1750 K, P = 39 ... 135 kPa.

Most of the experimental data obtained are in the temperature range above 1200 K. The average error of the experimental data is 3%. From the experimental data on the viscosity of cesium and rubidium in the gas phase, the values of the effective cross sections of the «atom-atom» collisions and

[1] Candidate of Technical Sciences,
Associate Professor of the Department of Mathematics, Physics and Computer Technologies,
Vinnytsia National Agrarian University, Ukraine
[2] Assistant of the Department of Mathematics, Physics and Computer Technologies,
Vinnytsia National Agrarian University, Ukraine

the relative cross-sections of the «atom-molecule» collisions were obtained. Calculated equations and tables of viscosity and thermal conductivity of cesium and rubidium vapor in the temperature range 700-2000 K and pressures 1-1500 kPa, including the saturation line, have been developed.

An experimental study of the viscosity of rubidium and cesium vapor at high temperatures have been conducted with implementation of the method from a viscosimeter with an annular channel. From the experimental data on the viscosity of cesium and rubidium in the gas phase, the values of the effective cross sections of the «atom-atom» collisions and the relative cross-sections of the «atom-molecule» collisions were obtained. Calculated equations and tables of viscosity and thermal conductivity in a wide range of temperatures and pressures have been developed.

1. Introduction

The alkali metal vapor in the state parameters T = 700… 2000K, P = 1… 1500 kPa available for experimental study consists of atomic and molecular components with a rather low concentration of clusters and charged particles. The concentration of diatomic molecules in a pair is unequivocally determined by the parameters of its state: pressure and temperature. Thus, the viscosity and thermal conductivity of alkali metals in the gas phase in the selected temperature range can be considered as the processes of transfer in a binary mixture of rarefied ideal gases, taking into account the course of dissociation reactions.

Theoretical methods for calculating the viscosity and thermal conductivity of alkali metal vapors are significantly limited due to the lack of sufficiently accurate data on the interaction potentials of «atom-atom», «atom-molecule»and «molecule-molecule». The experiment is still the only source of information necessary for the transfer coefficients of alkali metal vapor.

Experimental studies of alkali metal vapor transfer processes are associated with difficulties in the implementation of experimental methods due to the high chemical activity of alkali metals at high temperatures, and with the study of cesium there appear a number of additional complications associated with its specific properties. In real conditions of the experiment, the processes associated with thermoelectron emission and surface ionization, photoeffect and photoionization can occur, at high temperatures

the number of inelastic collisions of atoms increases, and at high pressures the reality of gases manifests itself. However, it is possible to create such experimental conditions in which the listed effects are not noticeable, and to identify the vapor state region in which the ideal gas model can be used to describe the transfer phenomena, in which molecule formation and decay reactions take place, which allows to apply the results of strict kinetic Chapman-Jensky and Hirschfelder-Brokau theories [1] for a mixture of reacting gases and its specific application for alkali metal vapors [2; 3].

The aim of this work is to establish the dependence of viscosity and thermal conductivity of rubidium and cesium in the gas phase on temperature and pressure and to construct calculation equations and tables of viscosity and thermal conductivity in a wide range of temperatures and pressures.

2. Research method

Experimental methods previously used to study the vapor viscosity of alkali metals, except for the method of a viscometer with an annular channel [5; 6; 8], are limited to a temperature of 1200-1300 K.

The annular-channel viscometer method allows experiments with alkali metal vapors at temperatures well above 1200 K. It was first used by V.I. Dolgov [8] to study the viscosity of lithium vapor. In [8] the advantage of this method over the previously used methods of measuring the viscosity of alkali metal vapors is shown, its disadvantages are considered. I.F. Stepanenko [5] improved this method, developed the original design of the measuring cell. In [6] the flow of alkali metal vapor in the working gap of the viscometer was analyzed, the method of calibration of the measuring element and measurement of condensate flow was improved, accuracy was significantly increased, lithium vapor viscosity T = 1595 ... 1983 K, P = 15 ... 107 kPa and sodium at T = 1109 ... 1524 K, P = 12 ... 100 kPa was researched.

At temperatures up to 2000 K and pressures of 1 ... 1500 kPa, alkali metals in the gas phase can be considered as a binary gas mixture consisting of atoms and diatomic molecules, between which dissociation reactions take place.

Theoretical methods for calculating the viscosity and thermal conductivity of alkali metal vapor as a reactive gas mixture of atoms and diatomic molecules are significantly limited due to the lack of accurate

data on the potentials of «atom-molecule» and «molecule-molecule» interaction. Existing calculation methods are connected with a number of simplifications that reduce the results of such calculations to the level of estimates. The experiment is still the only source of information necessary for the transfer coefficients of alkali metal vapor. Theory [2; 3] makes it possible to obtain the values of the relative cross sections of the atom-atom and atom-molecule collisions from experimental viscosity data and, using them, to calculate the coefficients of thermal conductivity and vapor viscosity in a wide range of state parameters.

One of the most convenient experimental methods for studying the viscosity of alkali metal vapor is the annular-channel viscometer method. In such a viscometer, an alkali metal vapor flows through a channel between two coaxial cylinders. This design of the viscometer makes it possible, in relation to classical capillary methods, to reduce by an order of magnitude the linear dimensions of the working element, which ensures the stability of the vapor temperature and the stability of its composition along the working element.

An experimental installation for the study of the viscosity of alkali metals was developed on the basis of [5; 6; 8]. It is a closed circulation circuit, the high-temperature part of which is made of niobium-zerconium alloy, and the low-temperature part of stainless steel. The measuring element of the cell is an annular channel formed by two coaxial cylinders. The measuring cell is equipped with a drip device that provides high stability of the steam generator. The design of the viscometer allows you to directly measure the temperature of the inner part of the measuring element of the viscometer, which improves the accuracy of determining the temperature of steam in the annular gap of the cell.

Schematic diagram of the installation is shown in Figure 1.

The measuring cell of the installation (elements 1-7) is placed in the vacuum chamber 8. The cell consists of an evaporator I, a viscometer (elements 2, 3), a superheater 4, a pressure tube 5, a refrigerator 6, a drip device 7. The working element of the viscometer is an annular gap formed between the inner surface of the pipe 2 and the cylindrical insert 3. The temperature of the evaporator is maintained by the heater 9, and of the viscometer by the heater 10. The cell has a system of thermal screens II, consisting of two packages of end and three packages of radial screens. The

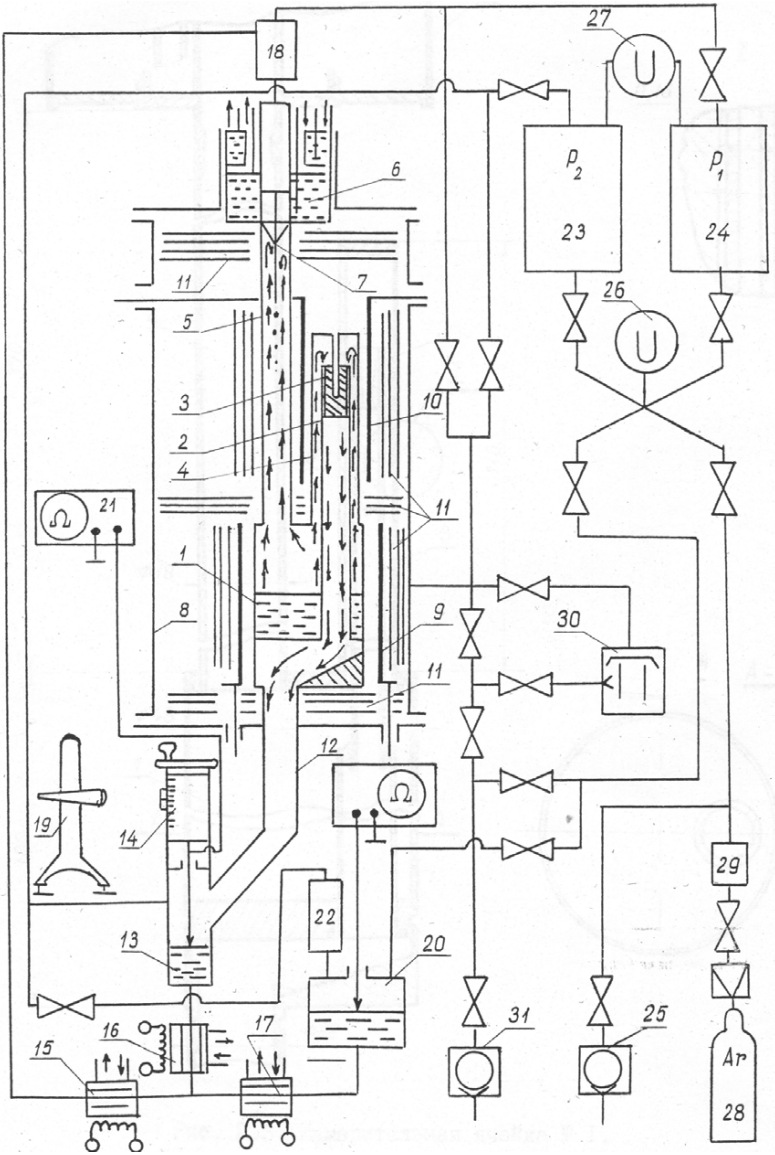

Figure 1. Schematic diagram of the installation

upper and lower flanges of the vacuum chamber are connected to its body by means of a ditch – wedge connection. A condensate collection line 12 is welded to the lower flange of the chamber. A measuring cell is connected to its upper part by means of a vacuum connection «ball-cone», and a flow meter 13 is attached to the lower part of the cell, equipped with a device for fixing small movements of the flowmeter needle 14.

The flowmeter is connected to a system of liquid taps 15, 16, 17, by means of which the drain vessel 20 is connected to the flowmeter or ballast vessel 18. The displacement of the flowmeter needle is measured by a catheter 19, the moment of contact with the needle of the surface of the liquid metal in the flowmeter is measured by the value of the electrical resistance resistance «needle – flow meter». The drain vessel is connected to the filling device 22 through the pipe 31.

The housing, upper and lower flanges of the vacuum chamber are cooled by water. The «ball-cone» vacuum connection of the cell is cooled by means of a copper heat sink connected to the lower flange of the chamber.

The gas system consists of receivers 23, 24 and a high-vacuum pump 25. It serves to create the working pressure in the measuring cell and the pressure drop in the area of the viscometer. The argon pressure in the system is measured by a mercury ∪-like manometer 26, and the pressure drop between the receivers by an oil ∪-like manometer 27, the atmospheric pressure is measured by a mercury manometer (ICB type – 1).

Argon in the gas system of the installation comes from the cylinder 28 through the gas filter 29 filled with liquid alkali metal (respectively Cs or Rb).

High vacuum P $\approx 1 \cdot 10^{6}$ millimetres of mercury column) in the chamber 8, and if necessary in the receivers 23, 24 is created by a high-vacuum system consisting of a vacuum diffusion pump 30 and a vacuum mechanical pump 31.

The measuring cell, gas and vacuum systems are interconnected by stainless steel pipes and switched together by means of vacuum valves.

Electric heaters 9, 10 are made of molybdenum foil, powered by AC mains through low-voltage transformers, the primary voltage of which is set by a voltage regulator.

The principle of operation of the installation is as follows: the investigated metal vapor comes from the steam generator to the steam heater, passes

through the measuring element of the viscometer, condenses in the cold part of the condensate collection line and is collected in the flow meter. The pressure drop on the measuring element is created through the intermediate inert gas – argon.

The viscosity of the vapor is determined by the mass flow rate of the alkali metal through the annular channel at a given value of the pressure drop across the measuring element of the viscometer. To do this, the installation must ensure high stationary flow of steam in the annular channel at constant values of temperature and pressure of the experiment.

Two measuring cells (Figures 2, 3), which differ in the design of the viscometer, were used in the work. The measuring cell consists of an evaporator 1, a viscometer (elements 2, 5), a superheater 3, a pressure pipe 4, a refrigerator 6 with a drip device 7.

The working element of the viscometer is an annular channel formed between the inner surface of the pipeline 2 and the cylindrical insert 5. The dimensions of the annular channels of the cells are given in table 1.

Table 1

Cell	№ 1	№ 2
Internal diameter of a pipe, mm	5,00 ± 0,01	6,05 ± 0,01
Diameter of a cylindrical insert, mm	4,68 ± 0,01	5,73 ± 0,01
Length of a working site, mm	26,0 ± 0,1	32,0 ± 0,01

The cylindrical insert of the cell № 2 differs from the cylindrical insert of the cell № 1 (Figures 4, 5) by the geometry of the inlet section, the method of attachment and has a recess for installing the thermocouple.

The cylindrical insert of the cell № 1 was inserted into the tube 2, the upper struts were welded to its ends. In the cell № 2 the cylindrical insert was inserted into the pipe 2 and welded to the end of the pipe 3, the upper and lower locking protrusions slide freely on the surface of the pipe.

All parts of the measuring cell, except for the refrigerator and the needle of the drip device, are made of niobium alloy NbCU and are interconnected by electron beam welding.

The body of the refrigerator is made of stainless steel, the stainless steel-niobium connection is made in the cold zone (T < 320 ... 400 K), which eliminates mechanical loads on the welded joint due to thermal expansion.

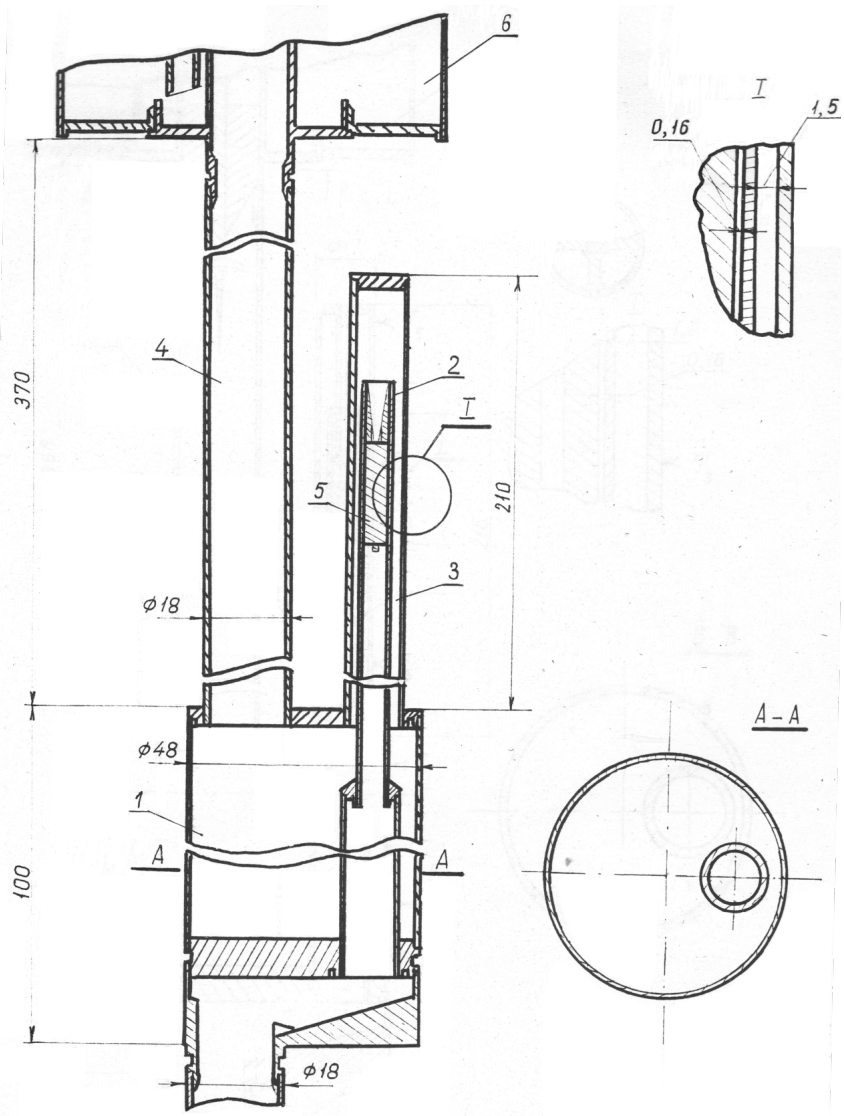

Figure 2. Measuring cell № 1

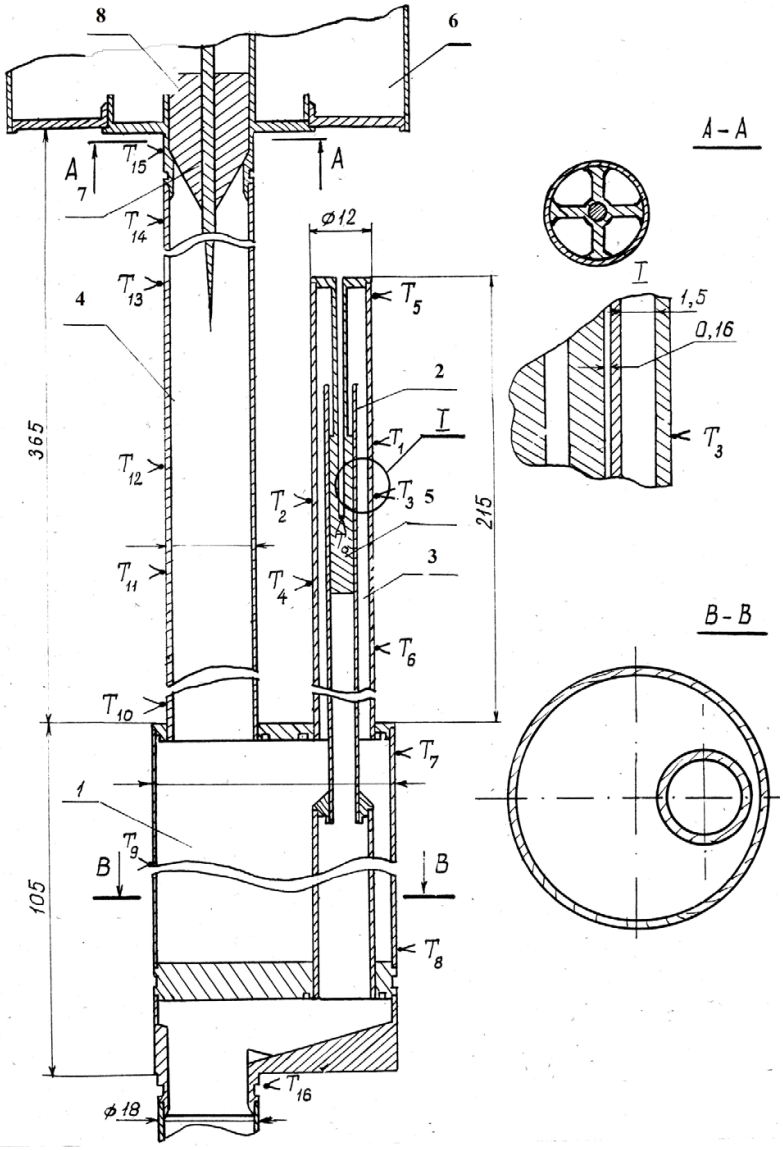

Figure 3. Measuring cell № 2

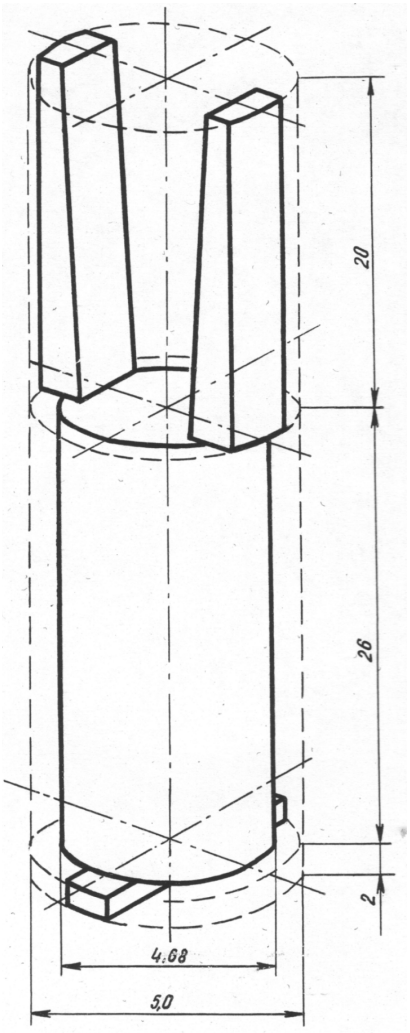

Figure 4. Cylindrical insert of the measuring cell № I

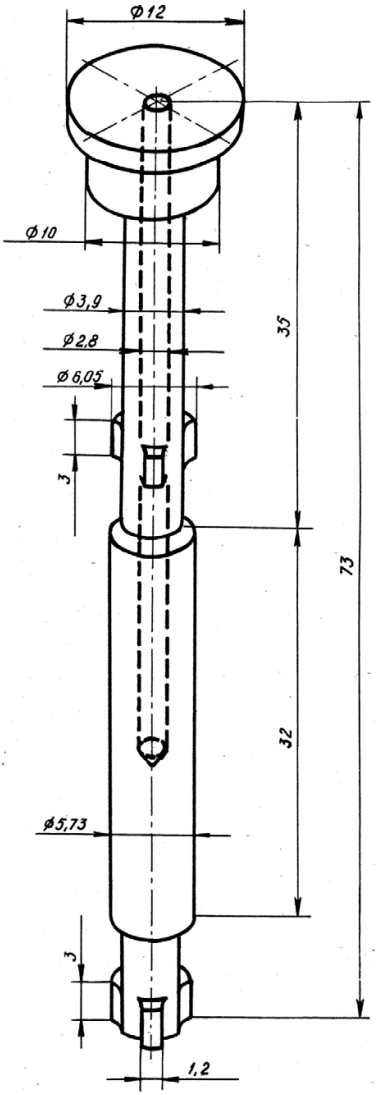

Figure 5. Cylindrical insert of the measuring cell № 2

The refrigerator of the measuring cell has two sections: low-temperature (water-cooled), designed to cool the vacuum seal cell-upper flange of the vacuum chamber and high-temperature (T ~ 400 K), cooled with silicone oil PFMS-4, designed to cool the drip devise.

The drip device (elements 7, 8, Figure 3) is used for condensation and return of liquid alkali metal in small portions (in the form of drops) to the steam generator 1. It is a needle-shaped tungsten rod 7, fixed by molybdenum heat sink 8 in the refrigerator area. The cell temperature was measured at control points T1 – T16 by tungsten – rhenium thermocouples BP5 / 20-I.

Liquid cranes are intended commutation of mains with alkali metal. They are (Figure 6) two coaxial tubes 1, 2 with an electric heater 3. In the main 1 is an alkali metal. The outer tube 2 can be cooled by water or heated by an electric heater 3.

In the cold state in the inner tube 1 a plug of crystalline alkali metal is formed – the valve is closed, when heating the section of the main above the melting point the plug is eliminated – the valve is open.

The real geometric factor of the viscometer with an annular channel differs from the calculated one. This is due to a number of reasons: tolerances to the size of the elements, the presence of fasteners and centering elements, the displacement of the elements of the viscometer due to thermal deformation and dimensional changes when heated. Therefore, to

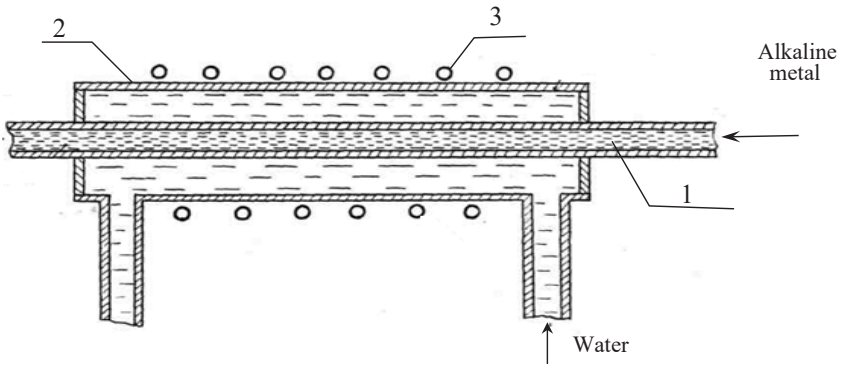

Figure 6. Liquid tap

determine the real value of the geometric factor of the measuring element, it is necessary to calibrate the viscosity of well-studied gases. In addition, the local loss factor remains unknown, which depends on the Reynolds number, geometric dimensions and shape of the annular channel. Theoretically, it is almost impossible to calculate the value. In most cases, it is determined by the results of calibration experiments [52; 53].

To determine the characteristics of the measuring element of the viscometer, stationary and non-stationary calibrations of measuring cells were performed.

Stationary calibration allows to determine the real value of the geometric factor *f* of the viscometer of the measuring cell, as well as to obtain the dependence *f* (*Re*), which takes into account the loss of kinetic energy at the entrance to the measuring channel [6].

Calibration was performed at atmospheric pressure by the method of stationary purge of the measuring element with standard gases (dry air, argon).

The viscosity η_{st} of standard gases is taken from [54]. The Reynolds number was calculated by a known ratio:

$$R_e = \frac{2\rho v\sigma}{\eta},$$

where $\sigma -$ the gap value of the channel, $v -$ the average gas flow rate in the channel.

Before calibration, each measuring cell was annealed in vacuum at a pressure of P = $1 \cdot 10^{-5}$ millimeters of mercury column and temperature T = 1800 ..... 1900 K for 2-3 hours. Stationary calibration was performed before and after experiments with alkali metal vapors. For calibration cell № 1 calibration 4 experiments were performed, and for cell № 2-5. Calibration experiments were performed in a wide range of Reynolds numbers (*Re* = 10...220), at a close value of Re were taken 3-7 experimental points, and their total number in the series ranged from 30 to 150. The obtained experimental values of the geometric factor *f* were approximated by a linear dependence $f = f_0 + A \cdot Re.$

The calibration results are shown in table 2, where: N is the number of experimental values, $\frac{\Delta f}{f}$ _ the relative value of the relative error, %.

Based on the results of stationary calibration, the following conclusions can be drawn:

1. Geometric factors of measuring cells did not change during experiments with alkali metal vapors.

2. The loss of kinetic energy at the entrance to the measuring channel clearly depends on the Reynolds number. The value of the geometric factor, taking into account local losses in the range of Reynolds numbers $Re = 0 \ldots 200$ decreases for cell № 1 by 6 %, and for cell № 2 by 2%.

The geometric factor of the measuring element of the viscometer with an annular channel also depends on the temperature. Its relative change (hereinafter the correction for thermal expansion is equal to:

$$\varepsilon_T = \frac{f_T}{f},$$

where f and f_T – the values of the geometric factor at the temperature of T_0 and T.

Table 2

The results of stationary calibration of the measuring cells

$$f \cdot 10^{12} = f_0 + A \cdot Re, m^3$$

Cell №	f_0	**A·10⁴**	N	$\frac{\Delta f}{f}$ **%**	Re	**Gas**	**Calibration time**
1	1,206	2,85	146	0,56	10…220	Air	Before experiments with cesium
1	1,221	3,17	47	0,74	16…178	Argon	
1	1,209	2,90	26	0,80	20…166	Argon	After experiments with cesium
1	1,218	3,33	94	0,64	18…200	Air	
1	1,214	3,00	313	0,46	10…220		Generalized meaning
2	0,660	0,649	87	0,72	22…205	Air	Before experiments with cesium
2	0,666	0,679	58	0,78	26…110	Argon	
2	0,668	0,685	104	0,66	28..210	Air	After experiments with cesium, before experiments with rubidium vapor
2	0,660	0,633	43	0,88	20…85	Argon	
2	0,662	0,654	76	0,68	18…160	Air	After experiments with rubidium vapor
2	0,663	0,653	368	0,56	18…210		Generalized meaning

To determine the correction, non-stationary calibration of the measuring cells in the operating temperature range was performed (for the cell № 1 T = 800 ... 1500 K, for the cell № 2 T = 800 ... 1850 K). The correction was determined depending on the time of change of the pressure difference of the inert gas that passed through the measuring cell of the viscometer.

Non-stationary calibration of the measuring cells was performed on argon and neon of high purity. Since in the cell № 2 the cylindrical insert of the viscometer (Figure 3) can be shifted in the vertical direction when

Table 3

Results of non-stationary calibrations of the measuring cells

Cell, №	Interval temperatures, *K*	α	$b \cdot 10^5$	N	$\frac{\sigma\varepsilon_t}{\varepsilon_t}$, %	Gas	Calibration time
1	800…1500	1,034	7,75	59	0,80	argon	Before conducting experiments with cesium vapor
1	800…1430	1,042	7,53	21	0,98	neon	
1	800…1360	1,046	7,69	33	0,86	argon	During experiments with cesium vapor
1	820…1400	1,038	7,57	64	1,10	argon	After conducting experiments with cesium vapor
1	800…1500	1,040	7,62	177	0,77		Generalized meaning
2	790…1850	1,170	2,81	81	0,76	argon	Before conducting experiments with cesium vapor
2	830…1840	1,163	2,98	33	0,92	neon	
2	850…1800	1,159	3,06	42	0,86	argon	During experiments with cesium vapor
2	810…1850	1,172	2,73	48	0,73	argon	After experiments with cesium vapor, before experiments with rubidium vapor
2	960…1810	1,175	2,80	37	1,02	argon	During experiments with rubidium vapor
2	920…1500	1,165	2,90	40	0,86	argon	During experiments with rubidium vapor
2	790…1850	1,168	2,85	281	0,63		Generalized meaning

the cell is heated, the amount of correction ε_t can change with increasing evaporator temperature. Therefore, for the cell № 2 additional calibration experiments were performed at different temperatures of the steam generator.

As can be seen from Figure 1, non-stationary calibration can be performed on the main experimental installation. This allows you to control the value of the geometric factor *f* during experiments with vapors of alkali metals, without disassembling the installation. To do this, the alkali metal during the experiment was completely distilled from the steam generator into the flow meter, where it was frozen, and then there was conducted, according to the previously described method, a series of reference and control experiments.

In the temperature range T = 800 ... 1850 K (for the cell № 1 T = 800 ... 1500 K) the dependence is described within the error of calibration experiments by linear dependence:

$$\varepsilon_t = a + bT.$$

The calibration results are shown in table 3, where *N* – the number of experimental points; $\frac{\sigma\varepsilon_t}{\varepsilon_t}$ – standard, %.

The relative changes ε_t in the corrections for the cells in the operating temperature range are:

– for the cell № 1 $(\varepsilon_{1500} - \varepsilon_{800}) / \varepsilon_{800} = 4,8\%$;

– for the cell № 2 $(\varepsilon_{1850} - \varepsilon_{800}) / \varepsilon_{800} = 2,5\%$.

Corrections for thermal expansion $\varepsilon_t(T)$ for both measuring cells changed monotonically, no hysteresis dependences $\varepsilon_t(T)$ were observed.

3. Experimental part

Alkali metal in the glass ampoules was placed in the refuelling device 19 (Figure 1). The working volume of the installation was pumped to a pressure of P ~ 10^{-5}–10^{-6} millimetres of mercury column). The gas system, flow meter, drain and ballast vessel were heated to a temperature of 400 ... 500 K. The working volume of the installation was «washed» several times with argon, and then filled with high purity argon (P = 100 kPa). The pressure in the receivers 22 and 23, the cell, the filling device and the drain vessel was equalized. The temperature of the drain vessel and the filling device was maintained at 60-80 ° C above the melting point of the alkali metal.

With the closed liquid taps 15 and 17 in the filling device the glass ampoule with alkali metal is crushed, and liquid alkali metal flows into the drain vessel. The level of metal in the drain vessel is controlled by a contact needle. The flowmeter is heated, the liquid tap 17 is opened. Excess pressure of argon is created – between the drain vessel and the flowmeter, then the initial level of alkali metal in the flowmeter is exposed. The liquid valve 17 is closed. The drain and ballast vessels, the main pipeline 29, the steam generator, the pressure pipe, the refrigerator of the measuring cell are heated. The liquid tap 16 opens. Excess argon pressure is created between the drain and ballast vessels. With excess pressure, the alkali metal is first distilled into the ballast vessel 18, and from there flows into the steam generator 1 of the measuring cell. Liquid valves 15 and 16 are closed, the pressure in the gas system is equalized.

The alkali metal vapor elasticity curve $P=f(T)$ [51] determines the temperature T and the vapor saturation pressure P_S of the investigated alkali metal, which corresponds to the planned parameters of the experiment. In the gas system of the installation argon P_{Ar} pressure is created, which is slightly higher P_S. The flow meter, the condensate collection path (T = 400 ... 450 K) and the refrigerator of the measuring cell (T = 300 ... 400 K) are heated.

The boiler (steam generator) and the viscometer of the measuring cell are adjusted at the appropriate temperature T_K, T_B. When $P_{Ar} > P_S$ liquid alkali metal is «crushed» by argon. The pressure in the gas system is slowly released. When $P_{Ar} = P_S$ the process of boiling alkali metal in the steam generator of the measuring cell begins. Hot alkali metal vapor fills the pressure pipe. The boiling moment is recorded by the readings of thermocouples $T_{10}…T_{15}$ installed on the height of the pressure pipe of the measuring cell (Figure 7).

The alkali metal vapor column displaces argon from the hot zone of the pressure pipe into the refrigerator zone. There is no alkali metal vapor in the cold zone of the pressure pipe and argon in the hot zone. Thus, the alkali metal vapor is «locked» by argon, i. e. we have the ability to regulate the alkali metal vapor pressure through the intermediate inert gas. This method of setting the pressure has been repeatedly used in thermal and spectrophysical experiments with alkali metal vapors [6; 24; 27; 34] and has shown high reliability.

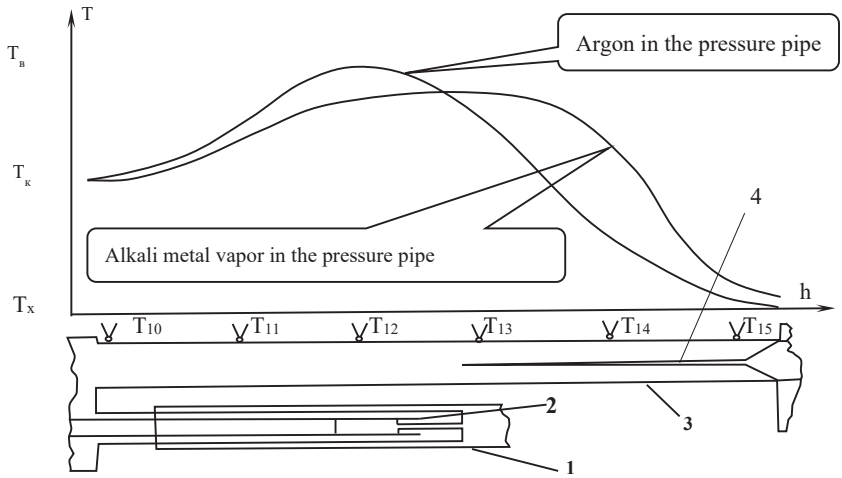

Figure 7. Temperature distribution by the height of the pressure pipe: 1 – heater, 2 – viscometer, 3 – pressure pipe, 4 – drip device, T10-T15 thermocouple BP5 / 20

Alkali metal vapor condenses on the drip device. It then flows down the needle of the drip device into the upper part of the hot zone of the pressure pipe and in small portions (in the form of small drops) returns to the steam generator, partially evaporating in the counterflow of steam. The counterflow of steam also carries argon into the cold zone, which is released from the liquid alkali metal on the needle of the drip device. The alkali metal condenses on the refrigerator of the drip device and flows down the needle of the drip device down in small drops. It returns to the evaporator at a temperature close to the boiling point, which provides high stability of steam generation. As can be seen from Figure 7. drainage of alkali metal on the walls of the pressure pipe is impossible, because the wall temperature is much higher than its boiling point.

After stabilization of temperature modes of the installation between the receivers 22 and 23 (Figure 1) the pressure difference on the measuring element is set. Under the action of the pressure drop, alkali metal vapor passes through the end channel and condenses in the cold part of the condensate collection line, then flows into the flow meter. In the flowmeter,

the metal level is controlled by a contact needle. The contact needle is moved by the device of small displacements 14, the displacement of the needle is determined by the catheter 19 (Figure 1). Consumption of alkali metal is determined by the rate of filling the flow meter.

At stable modes of the operation of installation the speed of filling of the flowmeter $B = \Delta h/\tau$ (Δh-height of rise of level of condensate of the flowmeter for a period of time $\Delta\tau$) has to be constant, and dependence $h=f(\tau)$ – linear:

$$h = h_0 + B \cdot \tau.$$

To increase the accuracy of measuring the flow of alkali metal and control the process of condensate flow into the flow meter during the experiment, the coefficients h_0,B and their random errors were calculated $\delta h_0/h_0$, $\delta B/B$ [26; 63; 69]. The experiments were completed when the required accuracy of the coefficient was reached B (in most cases $\delta B/B < 1\%$. If this level was not reached, the measurement cycle was terminated due to the limited service life of the installation. Typically, condensate level measurements in the flowmeter were performed 5-15 times for each measurement cycle. After full consumption of the alkali metal of the steam generator, the liquid alkali metal was distilled from the flow meter into the drain vessel and then into the steam generator, and the measurement cycle was repeated at new parameter values.

Two series of the experiments with cesium vapor and one series of experiments with rubidium vapor were performed. The experiments were performed on isotherms, with the deviation of the points on the isotherm was 10 ... 15 K.

The first series of the experiments with Cs pairs was performed on the measuring cell №1 without a drip device. 46 experimental values of viscosity in the temperature range 900 ... 1250 K at pressures 12 ... 125 kPa were obtained [65; 69; 74]. At temperatures above 1300 K there was instability in the operation of the steam generator installation.

The second series of the experiments was performed with a measuring cell № 2, which is equipped with a drip device. The drip device provided high stability of the steam generator of the measuring cell in a wide range of temperatures and pressures. 121 experimental values of cesium vapor viscosity were obtained, the temperature range of 960 ... 1770 K at pressures

of 19 ... 135 kPa was investigated [59; 69; 70; 71; 72]. The installation worked stably.

Experiments with rubidium vapor were performed on the cell № 2, 61 experimental values of viscosity in the temperature range of 990 ... 1750 K at pressures of 39 ... 135 kPa were obtained [66; 72].

The temperature of the measuring element of the viscometer during the experiments was maintained with high accuracy. During the experiments, the temperature variation in the height of the working element of the viscometer was ± 2 ... 5 K (thermocouples T_0, T_1, T_2, T_3, T_4, Figure 7), the temperature change during the experiments did not exceed ± 2 ... 3 K. For the cell № 2, the difference between readings between thermocouples T_2, T_3 and central T_0, which is located inside the cylindrical insert of the viscometer, did not exceed 2 ... 3 K, i. e. was outside the accuracy of temperature measurement by thermocouples.

The temperature of the steam generator during the experiments was also quite stable. There was almost no change in the readings of thermocouples $T_7 - T_9$ over time during the experiment. The temperature difference in the height of the steam generator did not exceed 10 K. The high stability of the evaporator cell № 2 is primarily due to the high efficiency of the drip device.

The experiments used alkali metals of the following composition (according to the passports of the manufacturer):

cesium:

Cs ≥ 99,99 %; K < 0,002 %; Na < 0,0005 %; Ca < 0,005 %; Rb < 0,001 %;

rubidium:

Rb ≥ 99,97 % ; K < 0,003 %; Na < 0,0003 %; Cs< 0,03 %.

During the experiment, the state of the alkali metal in the installation was monitored by comparing the experimental viscosity values determined at close parameters at the beginning and the end of each series of experiments.

Calculation formula of the method:

$$\eta = \frac{\pi\mu}{24RTQ_m}\left(2P_2 + \Delta P\right)\Delta P^* f \varepsilon_T \varepsilon_\lambda, \tag{1}$$

$$\Delta P^* = \Delta P - \left(0.77\rho V^2 - \frac{\Delta P^2}{P_2}\right), \tag{2}$$

Where η – the dynamic viscosity of the alkali metal vapor, T – the vapor temperature, ΔP – the pressure drop across the measuring channel, Q_m – the mass flow rate, P_2 – the vapor pressure at the outlet of the measuring channel, μ – the molar mass, ρ – the vapor density, V – the average vapor flow rate measuring channel, f – geometric factor of the cell, ε_λ – correction for the molecular slip, ε_T – correction for the thermal expansion.

Given the composition of the pair, its molar mass is equal to:

$$\mu = \mu_0 \left(1 + x_2\right), \tag{3}$$

where x_2 – the molar fraction of molecules in the pair (1,63 – 1,65);

μ_0 – molar mass of the atom.

Mass costs of steam Q_m are:

$$Q_m = \rho_{\text{p}} \pi R_T^2 \frac{\Delta h}{\tau} = \rho_{\text{p}} \pi R_T^2 B, \tag{4}$$

where ρ_{p} – the density of the liquid phase of the alkali metal at the temperature T;

R_T – radius of the flowmeter at temperature T_p.

$$R_T = R\left[1 + \alpha \left(T_P - T_0\right)\right]$$

T_0 – flow meter calibration temperature;

R – temperature flow meter radius T_0;

α – coefficient of linear expansion.

The condensate density was determined from the data [63]:

$$\rho_{Cs} \cdot 10^{-3} = 1,9058924 + 0,29801989\tau - 0,02852953 1\tau^2 + 4,6810162\tau^3 + \\ + 4,0361819\tau^4 + 1,736613\tau^5 - 0,29684317\tau^6, \; kg/m^3 \tag{5}$$

$$\rho_{Rb} \cdot 10^{-3} = 1,3511203 + 1,5219888\tau - 5,4165931\tau^2 + 7,415271\tau^3 - \\ - 5,3606866\tau^4 - 1,9604833\tau^5 - 0,28895999\tau^6, \; kg/m^3 \tag{6}$$

where $= {}^{T_P}/_{1000}$

The alkali ρ metal vapor density was determined by the equation:

$$\rho_{\Pi} = \mu_0 \left(1 + x_2\right) \frac{\bar{P}}{RT_T}, \tag{7}$$

where $\bar{P}$ – the average pressure of the experiment $\bar{P} = P_2 + \frac{\Delta P}{2}$;

T_T – gas vapor temperature in the viscometer channel.

The effective values of the geometric factors f of the cells and the correction for the thermal expansion of the measuring elements ε_T were determined by the results of the calibrations:

for the cell № 1

$$f = (1{,}214 + 3{,}00 \cdot 10^{-4}\mathrm{Re}) \cdot 10^{-12}, m^3 \quad (8)$$

$$\varepsilon_T = 1{,}040 + 7{,}62 \cdot 10^{-5}, \mathrm{T}, \quad (9)$$

for the cell № 2

$$f = (0{,}663 + 6{,}53 \cdot 10^{-5}\mathrm{Re}) \cdot 10^{-12}, \ m^3 \quad (10)$$

$$\varepsilon_T = 1{,}168 + 2{,}85 \cdot 10^{-5}\mathrm{T}. \quad (11)$$

Reynolds numbers Re were determined by the equation (12),

$$\mathrm{R_e} = \frac{2\rho v\sigma}{\eta}, \quad (12)$$

where σ – the magnitude of the gap of the channe;

v – ge average gas flow rate in the chanel.

Correction ε_λ for the molecular slip by equation:

$$\varepsilon_\lambda = 1 + \frac{6\lambda}{\sigma}, \quad (13)$$

where λ – the average free path of the molecules is three temperatures T.

The contribution of the correction for the viscosity in rubidium vapors is 0,2-4,1 %, and for cesium – 0,2-3,1%.

The average free path length of atoms λ included in the equation (13) is equal to:

$$\lambda = \frac{\eta_1}{0.49\rho\bar{c}}, \quad (14)$$

where η_1 – the viscosity of a monoatomic pair, which in the first approximation was calculated by [2].

The average thermal velocity $\bar{A}$ of atoms is:

$$\bar{c} = \sqrt{\frac{8\mathrm{RT}}{\pi\mu}} \quad (15)$$

The average flow rate of steam in the channel was determined by the ratio:

$$\bar{v} = \frac{Q_m}{\rho S}, \quad (16)$$

where S – the cross-sectional area of the channel.

The constants used in the calculations:

1. Energy of the dissociation of molecules [5]:

$D^0_{0CS} = 44380 \pm 1000$ Дж/моль , $D^0_{0Rb} = 48570 \pm 1000$ J/mol.

2. Molar masses of the monoatomic components [53]:

$\propto_{Cs} = 132{,}9054$ kg/kmol, $\propto_{b} = 85{,}4673$ kg/kmol.

3. The oil density of U-manometers was determined experimentally by comparing the readings of oil, water and mercury manometers:

$\rho_м = 881 \pm 3$ kg/m^3 – for the cell № 1, i $\rho_м = 993 \pm 3$ kg/m^3 – for the cell № 2.

An experimental study of the viscosity of cesium vapor (T = 900-1770 K, P = 12-130 kPa, two series of experiments, 205 experimental values of viscosity) and rubidium (T = 960-1750 K, P = 35-135 kPa, obtained – 61 experimental value of viscosity) was carried out and the confidence interval of the error of the experimental values of viscosity at the confidence level of P = 0,95 is in the range of 2,5 – 3,6% and averages 3%.

Table 4

Experimental values of cesium viscosity in the gas phase

№	*T*, К	*P*, kPa	$\eta \cdot 10^7$, *Pa · S*	X_2, %	Δε, %	№	*T*, К	*P*, kPa	$\eta \cdot 10^7$, *Pa · S*	X_2, %	Δε, %
1	**2**	**3**	**4**	**5**	**6**	**7**	**8**	**9**	**10**	**11**	**12**
I series of experiments						I series of experiments					
1	903	12,0	265,5	1,49	3,9	44	1227	42,9	330,0	0,98	3,9
2	906	13,4	264,4	1,62	3,1	45	1233	25,6	342,7	0,57	3,1
3	911	15,8	263,5	1,84	3,1	46	1254	48,7	348,1	1,00	3,0
4	917	26,5	264,0	2,90	3,7	II series of experiments					
5	916	40,4	253,6	4,31	2,7	1	964	60,7	269,6	4,70	3,4
6	914	40,2	251,2	4,34	3,5	2	972	80,1	263,8	5,78	2,8
7	916	48,6	252,2	5,10	2,8	3	973	27,3	273,4	2,11	2,8
8	921	56,2	246,0	5,64	3,4	4	974	30,5	277,7	2,34	2,7
9	924	52,1	250,2	5,17	4,2	5	975	44,2	271,9	3,30	2,7
10	920	51,7	251,2	5,27	3,2	6	975	36,2	273,6	2,73	2,8
11	972	86,4	264,8	6,18	2,8	7	975	20,8	282,6	1,61	2,9
12	973	43,7	273,0	3,30	2,9	8	977	71,0	265,2	5,05	2,7
13	1038	46,7	288,2	2,47	2,7	9	977	88,3	263,2	6,13	2,7
14	1057	73,8	288,9	3,46	4,3	10	978	58,0	268,5	4,17	2,8
15	1056	91,5	286,3	4,24	2,8	11	978	33,7	276,3	2,51	2,8

(Continuation of the Table 4)

1	2	3	4	5	6	7	8	9	10	11	12
16	1040	20,1	310,5	1,08	4,3	12	978	93,9	264,6	6,44	2,7
17	1040	67,1	286,7	3,45	2,8	13	980	74,4	269,2	5,18	2,7
18	1031	52,2	288,7	2,85	3,5	14	1040	70,8	284,6	3,62	2,8
19	1054	88,0	287,0	4,13	3,0	15	1046	38,0	293,7	1,95	2,8
20	1052	108,7	278,8	5,06	3,5	16	1047	106,9	283,0	5,11	3,1
21	1048	39,0	295,4	1,98	3,0	17	1048	75,8	291,0	3,71	2,6
22	1055	76,5	282,5	3,61	4,5	18	1048	43,7	296,2	2,20	2,8
23	1052	122,6	275,1	5,64	2,8	19	1049	54,5	290,0	2,71	3,1
24	1059	101,0	280,6	4,58	2,9	20	1049	133,7	278,1	6,18	2,7
25	1057	76,6	282,7	3,58	2,7	21	1050	84,5	280,2	4,06	3,5
26	1045	47,7	284,8	2,43	3,2	22	1052	122,1	272,0	5,62	2,9
27	1128	119,7	304,2	3,92	3,0	23	1068	80,3	292,2	3,55	2,8
28	1129	87,3	299,0	2,91	3,4	24	1128	58,6	305,7	2,00	2,7
29	1139	66,8	307,5	2,16	3,0	25	1129	112,7	305,9	3,69	2,7
30	1121	50,8	306,0	1,80	3,1	26	1129	45,3	316,6	1,55	3,5
31	1134	18,4	318,0	0,63	2,9	27	1130	86,4	309,1	2,89	2,9
32	1138	29,2	307,3	0,97	3,2	28	1134	75,9	312,5	2,49	2,7
33	1143	74,8	313,4	2,36	3,3	29	1134	41,1	312,4	1,38	3,2
34	1152	52,6	308,5	1,62	3,2	30	1136	103,2	312,4	3,30	2,7
35	1133	132,9	395,6	4,23	2,7	31	1138	58,0	318,0	1,89	3,2
36	1143	112,8	300,2	3,48	3,0	32	1144	72,6	310,8	2,29	2,7
37	1139	69,8	303,6	2,25	2,7	33	1225	98,8	333,1	2,21	2,7
38	1139	31,4	316,1	1,04	2,9	34	1225	76,4	341,4	1,73	2,8
39	1245	109,8	330,3	2,27	3,3	35	1226	106,7	325,3	2,37	3,2
40	1235	132,2	323,7	2,81	2,9	36	1228	66,8	349,0	1,50	2,8
41	1234	116,9	325,3	2,51	2,9	37	1229	131,6	332,5	2,86	2,7
42	1239	91,2	334,2	1,94	2,8	38	1231	51,3	348,9	1,15	2,7
43	1240	107,1	319,6	2,26	3,0	39	1231	124,8	336,6	2,70	2,8
40	1231	29,4	346,0	0,66	3,4	81	1499	113,8	410,1	1,04	2,7
41	1233	58,0	343,8	1,28	2,8	82	1500	35,9	432,1	0,33	2,8
42	1234	39,5	348,7	0,88	2,8	83	1501	75,0	418,7	0,69	3,0
43	1236	115,4	347,6	2,46	3,0	84	1503	94,0	410,0	0,86	3,1
44	1236	85,7	340,5	1,85	2,8	85	1504	30,5	430,7	0,28	2,8
45	1237	43,8	343,3	0,96	3,8	86	1504	134,1	414,3	1,21	2,8
46	1239	38,0	349,0	0,83	2,7	87	1505	57,9	420,1	0,53	3,2

(End of Table 4)

1	2	3	4	5	6	7	8	9	10	11	12
47	1325	39,0	375,5	0,62	2,9	88	1506	98,8	426,3	0,89	2,7
48	1326	79,7	372,7	1,25	3,0	89	1508	43,8	426,4	0,40	2,8
49	1328	80,2	367,7	1,25	2,6	90	1508	131,3	423,3	1,17	2,9
50	1328	100,6	367,0	1,56	3,1	91	1508	121,3	410,2	1,09	3,0
51	1329	113,8	366,6	1,75	3,4	92	1510	83,4	427,2	0,75	2,6
52	1329	133,8	364,1	2,04	2,8	93	1513	47,8	430,1	0,43	2,6
53	1329	120,7	366,8	1,85	3,4	94	1596	58,8	459,4	0,42	2,8
54	1330	88,1	367,5	1,36	2,7	95	1597	117,3	450,6	0,83	2,9
55	1330	58,5	372,9	0,91	4,2	96	1598	114,3	446,0	0,81	2,6
56	1332	58,0	368,3	0,90	2,8	97	1598	19,4	435,1	0,14	2,7
57	1332	43,5	371,4	0,68	2,9	98	1600	90,9	448,1	0,64	2,8
58	1334	72,6	372,0	0,11	2,9	99	1601	106,4	457,1	0,75	2,7
59	1334	48,7	368,7	0,75	3,3	100	1603	99,3	452,1	0,70	3,4
60	1335	31,2	376,3	0,48	4,2	101	1605	83,8	451,9	0,59	2,6
61	1335	127,0	373,3	1,90	2,7	102	1607	72,0	442,9	0,50	2,9
62	1336	44,2	377,1	0,68	3,2	103	1607	38,4	442,8	0,27	2,8
63	1337	99,1	374,2	1,49	2,7	104	1608	30,4	464,0	0,21	3,0
64	1338	69,2	370,1	1,05	2,8	105	1609	20,3	460,8	0,14	2,9
65	1343	91,9	372,2	1,36	2,7	106	1609	36,0	429,3	0,25	2,7
66	1350	121,2	367,2	1,73	3,4	107	1610	45,8	459,3	0,32	2,6
67	1427	57,3	395,8	0,65	3,1	108	1610	26,3	465,0	0,18	2,9
68	1429	98,8	391,6	1,11	3,2	109	1691	101,6	452,8	0,58	2,7
69	1429	130,4	392,8	1,46	2,7	110	1693	119,1	454,7	0,67	2,8
70	1430	68,0	404,0	0,77	2,9	111	1696	112,4	452,6	0,63	2,7
71	1430	120,5	395,8	1,34	2,9	112	1729	84,2	468,4	0,44	3,1
72	1430	28,8	404,6	0,33	2,7	113	1747	102,2	469,0	0,51	2,8
73	1431	73,2	387,0	0,82	2,9	114	1751	86,1	466,9	0,43	2,9
74	1433	113,8	397,5	1,26	2,8	115	1752	108,7	475,6	0,54	2,9
75	1434	20,0	413,9	0,28	2,9	116	1758	74,9	468,4	0,37	2,9
76	1435	89,3	402,8	0,99	3,0	117	1763	35,9	482,6	0,18	3,2
77	1437	117,4	405,6	1,28	3,1	118	1764	53,3	486,0	0,26	2,8
78	1446	95,8	405,3	1,03	2,6	119	1767	42,9	480,2	0,21	2,9
79	1498	100,9	424,5	0,93	3,3	120	1770	98,1	464,9	0,47	2,8
80	1498	71,3	416,8	0,66	2,8	121	1770	64,6	475,4	0,31	3,1

Table 5

Experimental values of rubidium viscosity in the gas phase

№	T, K	P, kPa	$\eta \cdot 10^7$, $Pa \cdot S$	X_2, %	$\Delta\varepsilon$, %	№	T, K	P, kPa	$\eta \cdot 10^7$, $Pa \cdot S$	X_2, %	$\Delta\varepsilon$, %
1	**2**	**3**	**4**	**5**	**6**	**7**	**8**	**9**	**10**	**11**	**12**
1	989	41,9	255,9	3,41	2,9	32	1312	111,2	335,4	1,87	2,7
2	995	114,2	235,9	8,10	3,0	33	1313	59,2	334,6	1,01	3,1
3	996	59,5	251,1	4,52	3,3	34	1322	135,9	323,7	2,19	2,9
4	998	105,6	232,1	7,45	2,7	35	1437	117,6	363,6	1,28	3,1
5	998	87,0	242,8	6,29	3,0	36	1438	108,9	372,5	1,19	3,1
6	1010	110,4	233,8	7,25	3,1	37	1440	75,5	355,7	0,82	3,0
7	1096	132,7	262,9	5,51	3,0	38	1443	90,2	361,2	0,97	3,0
8	1098	100,8	275,3	4,25	3,0	39	1444	118,1	358,7	1,26	4,2
9	1098	126,7	259,1	5,24	2,8	40	1444	39,6	364,7	0,43	3,2
10	1100	86,0	277,1	3,64	3,7	41	1445	135,9	354,2	1,44	3,1
11	1102	60,2	281,0	2,50	2,9	42	1447	65,3	369,2	0,70	3,0
12	1103	103,5	278,4	4,25	2,9	43	1447	52,8	366,0	0,57	3,7
13	1104	79,3	281,2	3,31	3,0	44	1449	56,2	364,7	0,60	3,2
14	1104	124,6	262,3	5,01	3,5	45	1450	39,6	372,0	0,42	3,0
15	1105	76,5	278,8	3,18	3,0	46	1452	46,8	361,1	0,49	3,9
16	1105	63,0	283,5	2,65	3,3	47	1563	106,3	409,0	0,80	4,0
17	1112	43,1	284,3	1,78	3,3	48	1563	104,6	400,4	0,79	3,1
18	1115	35,1	287,4	1,43	4,7	49	1578	121,5	400,7	0,87	3,6
19	1122	116,3	271,4	4,32	4,0	50	1580	90,4	404,3	0,65	3,2
20	1231	70,4	316,9	1,65	3,0	51	1582	126,3	396,8	0,90	3,1
21	1236	43,5	316,5	1,01	3,6	52	1583	102,5	401,3	0,73	3,1
22	1237	79,7	316,5	1,82	3,6	53	1584	80,2	414,0	0,57	3,5
23	1240	114,1	297,5	2,54	3,1	54	1584	134,8	401,6	0,95	3,1
24	1246	120,7	315,0	2,61	2,7	55	1591	125,7	400,2	0,87	3,0
25	1249	126,7	306,6	2,70	3,1	56	1734	105,3	451,9	0,51	3,1
26	1299	120,6	324,6	2,12	2,8	57	1736	80,3	450,4	0,39	3,9
27	1300	78,8	333,8	1,40	3,3	58	1739	134,0	442,4	0,64	4,2
28	1300	86,4	330,1	1,53	3,0	59	1740	94,9	453,5	0,45	2,9
29	1301	102,8	331,0	1,81	3,1	60	1746	123,8	445,5	0,58	3,0
30	1308	126,3	321,7	2,15	3,9	61	1751	125,4	449,1	0,58	3,3
31	1311	112,7	321,7	1,90	3,1						

where: T – alkali metal vapor temperature, K;

$\overline{P} = P_2 + \Delta P$ – average pressure, kPa;

η – experimental value of viscosity, $Pa \cdot s$;

ΔP – pressure drop at the measuring section, kPa;

x_2 – molar fraction of diatomic molecules in the alkali metal vapor, %;

$\Delta\varepsilon$ – the confidence limit of the error of the experimental value of the viscosity at a confidence level of P = 0,95.

The molar fraction of diatomic molecules was calculated according to [2].

$$x_2 = 1 - \frac{2}{1 + \sqrt{1 + \frac{4P}{1{,}01325K_p}}}, \quad (17)$$

where P – the pressure of vapour; K_p – equilibrium constant.

$$K_p = \exp\left\{\frac{2\Phi_1^* - \Phi_2^*}{R} - \frac{D_0^\circ}{RT}\right\} \quad (18)$$

where T – temperature vapour;

D_0° – dissociation energy of the molecules;

R – universal gas table;

Φ_1^* and Φ_2^* – respectively isobaric – isothermal potential of the atomic and molecular components [44]:

$$\Phi_i^* = f_0 + f \cdot \ln\chi + f_{-2} \cdot \chi^{-2} + f_{-1} \cdot \chi^{-1} + f_1 \cdot \chi + f_2 \cdot \chi^2 + f_3 \cdot \chi^3$$

where $\chi = T / 1000$, and the values of the coefficients f_i are given in table 6.

Table 6

Coefficients of equation 1.65 [44]

f_i	Cesium		Rubidium	
	$2\Phi_1^* - \Phi_2^*$		$2\Phi_1^* - \Phi_2^*$	
	298,6 < T ≤ 1500 K	1500 < T ≤ 6000 K	298,6 < T ≤ 1500 K	1500 < T ≤ 6000 K
f_0	121,649	444,587	112,349	370,373
f	17,1427	224,653	13,8048	190,8541
f_{-2}	-1,2241·10-3	-0,6190364	-1,0199·10-3	-0,6288884
f_{-1}	0,26749	27,35144	0,19684	25,54826
f_1	-271,4918	-790,859	-194,6768	-589,339
f_2	1062,86	644,888	750,05	419,334
f_3	-1694,904	-230,756	-1135,468	-129,528

For cesium and rubidium in the temperature range T = 900 ... 1800 K and pressures P = 10 ... 150 kPa at D°_{0cs} = 44380 J/mol, D°_{0Rb} = 48570 J/mol [45] the molar fraction of the molecules is x_2 = 0.1 ... 10 %.

4. Calculation of the collision cross sections

The viscosity of the alkali metal vapor can be expressed through two parameters [2]: the effective cross-sections of the «atom-atom» $\sigma_{11}^2\Omega_{11}^{(2,2)*}$ collisions and the relative cross-section of the «atom-molecule» β_{12}^2 collisions. The effective cross-sections of «atom-atom» $\sigma_{11}^2\Omega_{11}^{(2,2)*}(T)$ collisions characterize the dependence of the viscosity of a monoatomic pair on temperature, and relative β_{12}^2 – the dependence of viscosity on the concentration of the diatomic molecules, which is a function of pressure.

The viscosity of a two-component mixture is determined from the ratio [2; 3]:

$$\frac{1}{\eta} = \frac{X_\eta + Y_\eta}{1 + Z_\eta}, \tag{19}$$

$$X_Z = \frac{1}{\eta_1}x_1^2 + \frac{2x_1}{\eta_{12}} + \frac{1}{\eta_{22}}x_2^2, \tag{20}$$

$$Y_\eta = \frac{3}{5}A_{12}^*\left\{\frac{x_1^2 M_1}{\eta_1 M_2} + \frac{2x_1x_2}{\eta_{12}}\cdot\frac{(M_1+M_2)^2}{4M_1M_2}\frac{\eta_{12}^2}{\eta_1\eta_{22}} + \frac{x_2^2}{\eta_2}\frac{M_2}{M_1}\right\}, \tag{21}$$

$$Z_\eta = \frac{3}{5}A_{12}^*\left\{x_1\frac{M_1}{M_2} + 2x_1x_2\cdot\left[\frac{(M_1+M_2)^2}{4M_1M_2}\left(\frac{\eta_{12}}{\eta_1}+\frac{\eta_{12}}{\eta_{22}}\right)-1\right] + x_2^2\frac{M_1}{M_2}\right\}, \tag{22}$$

$$\eta_{ij}\cdot 10^7 = 26{,}693\frac{\sqrt{2M_iM_jT/(M_i+M_j)}}{\sigma_{ij}^2\Omega_{ij}^{(2,2)*}}, (i,j=1,2), Pa\cdot s, \tag{23}$$

$$\eta_{11}=\eta_1, \eta_{22}=\eta_{22}, \sigma_{11}^2=\sigma_1^2, \sigma_{22}^2=\sigma_2^2, \tag{24}$$

where M_1, M_2 – the mass of the atom and the molecule of the alkali metal, respectively;

x_1, x_2 – molar particles of the atoms and molecules;

η_1 – viscosity of the monoatomic gas;

η_2 –viscosity of the diatomic gas;

η_{12} –the viscosity of a hypothetical gas consisting of molecules by mass $2M_1M_2T/(M_1+M_2)$, interacting on the potential curve of the atom-molecule;

$\sigma_{ij}^2\Omega_{ij}^{(2,2)*}$ – effective cross sections of the gas particle collisions.

Given that $2M_1 = M_2$, and introducing the concept of the relative cross section of the particles $\beta_1^2, \beta_{12}^2, \beta_2^2$ V.S. Yargin [2; 3] for a pair of alkali metals received:

$$\eta_{cm} = \eta_1 \frac{1+b_{1\eta}\cdot x_2+b_{2\eta}\cdot x_2^2}{1+a_{1\eta}\cdot x_2+a_{2\eta}\cdot x_2^2}, \quad (25)$$

where

$$a_{1\eta} = 2\left(0{,}5\sqrt{3}\,\beta_{12}^2 + \frac{9\sqrt{6}}{40}A_{12}^*\beta_{12}^2\text{-}1\right)/\left(1+0{,}3A_{12}^*\right), \quad (26)$$

$$a_{2\eta} = -\left(a_{1\eta}+1\right)+0{,}5\sqrt{2}\,(1+1{,}2A_{12}^*)\beta_2^2/(1+0{,}3A_{12}^*), \quad (28)$$

$$b_{1\eta} = -1{,}8A_{12}^*\left(1-0{,}5\sqrt{2}\,\beta_{12}^2 - \frac{\sqrt{4}}{4}A_{12}^*\beta_1^2\right)/(1+0{,}3A_{12}^*), \quad (29)$$

$$b_{2\eta} = -b_{1\eta}+0{,}9A_{12}^*(1+0{,}3A_{12}^*), \quad (30)$$

$$\beta_{12}^2 = \frac{\sigma_{12}^2\Omega_{12}^{(2,2)^*}}{\sigma_1^2\Omega_{11}^{(2,2)^*}}, \quad (31)$$

$$\beta_1^2 = \frac{\sigma_{12}^2\Omega_{12}^{(2,2)^*}}{\sigma_2^2\Omega_{22}^{(2,2)^*}}, \quad (32)$$

$$\beta_2^2 = \frac{\sigma_2^2\Omega_{22}^{(2,2)*}}{\sigma_1^2\Omega_{11}^{(2,2)*}}, \quad (33)$$

$$\beta_{12}^2 = \beta_1^2\cdot\beta_2^2, \quad (34)$$

$$2\beta_{12}^2 = \beta_2^2+1, \quad (35)$$

Subsequently, given that the alkali metals in the gas phase, the molar fraction of molecules $x_2 << 1$, having decomposed (25) in a row on a small parameter x_2 in [2; 3], we obtained:

$$\eta(x_2, T) = \eta_1(T)\left(1+\sum_{n=1}^{m}A_n x_2^n\right) \quad (36)$$

where A_n it is determined by the ratios:

$$\left.\begin{aligned} A_1 &= -a_{1\eta}+b_{1\eta};\ A_2 = -a_{1\eta}A_1+b_{2\eta}\text{-}a_{2\eta} \\ A_n &= a_{1\eta}A_{n-1}\text{-}a_{2\eta}A_{n-2};\ n\geq 3 \end{aligned}\right\}, \quad (37)$$

Given that $A_{12}^* = 1{,}2$ [5; 22], we have:

$$a_{1\eta} = 1{,}2735\beta_{12}^2 + 0{,}9724\beta_1^2\text{-}2, \quad (38)$$

$$a_{2\eta} = -\left(a_{1\eta}+1\right)+1{,}286\beta_2^2, \quad (39)$$

$$b_{1\eta} = +1{,}5852 + 1{,}3754\beta_{12}^{-2} + 0{,}9724\beta_1^{-2} - 2\,, \tag{40}$$

$$b_{2\eta} = 0{,}794 - b_{1\eta}, \tag{41}$$

From (36) we have that the excess viscosity due to the contribution of the diatomic vapor molecules is:

$$\frac{\eta - \eta_1}{\eta_1} = \frac{\Delta\eta}{\eta_1} = \sum_{n=1}^{m} A_n x_2^n, \tag{42}$$

Limiting in the equation (42) the first term, we have:

$$\frac{\Delta\eta}{\eta_1} = A_1 x_2\,. \tag{43}$$

The first approximation (43) has a clear physical meaning: the viscosity phenomenon is determined by the cross sections of the «atom-atom» and «atom-molecule» collisions, and the difference between the viscosity of the mixture and the viscosity of a monoatomic pair is determined only by the relative cross sections of the «atom-molecule» collisions β_{12}^2. The sign A of the coefficient characterizes the effect of viscosity pressure (dependence of viscosity on pressure, i. e. on the concentration of molecules). If $A < 0$, then with increasing (greater pressure) viscosity increases $\Delta\eta > 0$. When $A < 0$ viscosity decreases with increasing pressure $\Delta\eta < 0$. If $A = 0$, regardless of the pressure, at the same time $\beta_{12}^2 = \beta_{12critikal}^2$. It follows from the equations (37) and (43):

$$\beta_{12critikal}^2 = 1.21, \tag{44}$$

The second term of the equation (42) takes into account the contribution of the intermolecular interactions that are determined β_{12}^2, and the third and subsequent terms of the equation refine the physical picture without making qualitative changes [3].

Thus, the obtained theoretical results determine the viscosity of the alkali metal pair as a function of the absolute cross sections of the «atom-atom» $\sigma_{11}^2\Omega_{11}^{(2,2)*}$ collisions and the relative «atom-molecule» collisions β_{12}^2. Thus, the series according to x_2 (42) is a very convenient mathematical tool that allows processing, comparison and analysis of the various experimental data on the viscosity of alkali metals in the gas phase.

The viscosity of a single-volume pair η_1 in a wide temperature range is linearly dependent on temperature:

$$\eta_1(T) = \eta_0 + A(T - 1000)\,. \tag{45}$$

The viscosity of a monoatomic pair $\eta_1(T)$ and the effective cross sections of the atomic $\sigma_{11}^2\Omega_{11}^{(2,2)*}(T)$ collisions are related by the ratio:

$$\eta_1(T)\cdot 10^7 = \frac{26,693\sqrt{\mu T}}{\sigma_{11}^2\Omega_{11}^{(2,2)*}(T)} \ . \quad (46)$$

To determine the unknown parameters η_0, A, β_{12}^2, you need to minimize the target function

$$F\left(\eta_0, A, \beta_{12}^2\right) = \sum_{i=1}^{N} \frac{1}{\Delta\eta_i^2}\left(\eta_i - \eta_{Ti}\right)^2 , \quad (47)$$

where η_i – is the experimental viscosity value, $\Delta\eta_i$ – is the i viscosity error, η_{Ti} – is the viscosity value calculated from the ideal dissociating gas scheme [2].

$$\eta_{Ti} = \left[\eta_0 + A(T-1000)\frac{1+b_{1\eta}x_2+b_{2\eta}x_2^2}{1+a_{1\eta}x_2+a_{2\eta}x_2^2}\right], \quad (48)$$

$\sigma_{11}^2\Omega_{11}^{(2,2)*}$ where x_2 – the molar fraction of diatomic molecules in the pair $a_{1\eta}, a_{2\eta}, b_{1\eta}, b_{2\eta}$ – coefficients determined by the cross sections of the collisions «atom-atom» and «atom-molecule» β_{12}^2 [2].

The results of minimizing the target function $F\left(\eta_0, A, \beta_{12}^2\right)$ for experimental data [59; 69] at the dissociation energy of molecules of cesium $D_{0\,Cs}^0 = 44380 \pm 1000$ J/mol [45] and rubidium $D_{0\,Rb}^0 = 48570 \pm 1000$ J/mol [45] are shown in the table 7.

Table 7

The results of the experimental data processing

Metal	Coefficients of the equation 3		β_{12}^2	$\Delta\eta$, %	ΔA, %	$\Delta\beta_{12}^2$, %
	$\eta_0 \cdot 10^7$, $Pa \cdot s$	$A \cdot 10^7$, $Pa \cdot s / K$				
Cs	292,4	0,256	2,2	1,8	2,4	5,2
Rb	268,4	0,233	2,3	2,1	3,0	6,5

The viscosity of a monoatomic pair in the temperature range 700-2000 K is described by the equations:

$$\eta_1(T)_{Cs} = 292,4 + 0,256(T-1000), \text{ Pa}\cdot\text{s} , \quad (49)$$

$$\eta_1(T)_{Rbs} = 268,4 + 0,233(T-1000), \text{ Pa}\cdot\text{s} . \quad (50)$$

Let's calculate the effective cross sections of the collisions of the atoms $\sigma_{11}^2\Omega_{11}^{(2,2)*}(T)$ for the pair *Cs* and *Rb*. According to the equation (5) we have:

T, K		700	900	1000	1100	1200	1300	1500	1700	1800
$\sigma_{11}^2\Omega_{11}^{(2,2)*}$, A^{o2}	*Cs*	37,8	34,6	33,3	32,1	31,0	30,1	28,4	26,9	26,3
	Rb	32,9	30,2	29.1	28,1	27,1	26,3	24,8	23,6	23,0

In the temperature range 700 ... 2000 K, the dependence of the effective cross sections of the «atom-atom» collisions on the temperature is approximated by the equations:

$$\left.\begin{aligned}\sigma_{11}^2\Omega_{11}^{(2,2)*}(T)_{Cs} &= 54.7 - 32.5\frac{T}{1000} + 13.29\left(\frac{T}{1000}\right)^2 - 2.22\left(\frac{T}{1000}\right)^3, \quad \overset{o}{A}^2 \\ \sigma_{11}^2\Omega_{11}^{(2,2)*}(T)_{Rb} &= 41.7 - 26.8\frac{T}{1000} + 10.50\left(\frac{T}{1000}\right)^2 - 1.69\left(\frac{T}{1000}\right)^3, \quad \overset{o}{A}^2\end{aligned}\right\}.$$

The dependence of the relative cross sections of the «atom-molecule» β_{12}^2 collisions on the temperature could not be established because the error $\Delta\beta_{12}^2$ is too large. It is easy to show that to reduce it to 5 %, it is necessary to significantly expand the investigated pressure range $\Delta P \sim 1...2$ *mPa* and increase the accuracy of the input experimental data of the alkali metal vapor viscosity to 1 ... 2 %, which is currently a rather complex scientific and technical problem.

5. Generalization of the experimental results

According to the theory of the transfer phenomena, the viscosity and thermal conductivity of the alkali metals in the gas phase are a function of the absolute cross sections of the collisions «atom-atom» $\sigma_{11}^2\Omega_{11}^{(2,2)*}$ and relative – «atom – molecule» β_{12}^2. Thus, the theory [2; 3] makes it possible to process, compare and analyze a variety of experimental data on the viscosity of the alkali metals in the gas phase.

The theory of the thermal conductivity of the chemically reactive gas mixtures is based on the fact that the thermal conductivity of such a mixture is given in the form [2]:

$$\lambda = \lambda_f + \lambda_r, \tag{51}$$

where: λ_f the component of the thermal conductivity without taking into account the effect of the chemical reaction on the heat transfer process (the frozen component of thermal conductivity), λ_r the component of the thermal

conductivity due the energy transfer as a result of the reactions («reaction» component of the thermal conductivity).

The «reaction» component of the thermal conductivity is [2]:

$$\lambda_r = \frac{D_{12}P}{T}\left(\frac{D_0(T)}{RT}\right)^2 \frac{x_1 x_2}{(1+x_2)^2}, \quad (52)$$

$$D_0(T) = D_0^0 + 2H_1(T) - H_2(T), \quad (53)$$

where D_0° the energy of dissociation at the temperature $T = 0$, $H_1(T)$ and $H_2(T)$ – the enthalpy of the atomic and molecular components at the temperature T.

The «frozen» component of the thermal conductivity of the alkali metal vapor is served as a sum

$$\lambda_f = \lambda_{tr} + \lambda_{int}, \quad (54)$$

where λ_{int} the thermal conductivity due to the internal degrees of freedom of the interacting particles; λ_{tr} thermal conductivity due to the energy transfer caused by the translational degrees of freedom.

According to [2]

$$\lambda_{int} = \frac{nD_{22}(C_{p,2} - \frac{5}{2}R)}{1 + \frac{x_1}{x_2}\frac{D_{22}}{D_{11}}}, \quad (55)$$

where $C_{p,2}$ the specific heat at cansed by the constant pressure, R cansed by the universal gas constant.

$$\frac{1}{\lambda_\Pi} = \frac{X_\lambda + Y_\lambda}{1 + Z_\lambda}, \quad (56)$$

$$X_\lambda = \frac{1}{\lambda_{11}}x_1^2 + \frac{2x_1x_2}{\lambda_{12}} + \frac{1}{\lambda_{22}}x_2^2, \quad (57)$$

$$Y_\lambda = \frac{1}{\lambda_{11}}V^{(1)} + \frac{2x_1x_2}{\lambda_{12}}V^{(Y)} + \frac{1}{\lambda_{22}}x_2^2V^{(2)}, \quad (58)$$

$$Z_\lambda = x_1V^{(1)} + 2x_1x_2V^{(Z)} + x_2^2V^{(2)}, \quad (59)$$

$$\lambda_{ij}\cdot 10^4 = 833\sqrt{\frac{T(M_1+M_2)}{2M_1M_2}}\frac{1}{\sigma_{ij}^2\Omega_{ij}^{(2,2)*}}\ (i,j=1,2), W/(m\cdot K), \quad (60)$$

where:

$$\left.\begin{aligned} V^{(Y)} &= 0{,}3A_{12}^{*}\frac{\lambda_{12}^{2}}{\lambda_1\lambda_2} - V^{(3)} \\ V^{(1)} &= \frac{4}{15}A_{12}^{*} + \frac{1}{10}B_{12}^{*} + \frac{5}{24} \\ V^{(2)} &= \frac{4}{15}A_{12}^{*} - \frac{2}{5}B_{12}^{*} + \frac{1}{12} \\ V^{(3)} &= \frac{1}{5}B_{12}^{*} + \frac{3}{16}\frac{B_{12}^{*}}{A_{12}^{*}} + \frac{25}{64}\frac{1}{A_{12}^{*}} + \frac{1}{12} \\ V^{(4)} &= \frac{4}{15}A_{12}^{*} + \frac{1}{5}B_{12}^{*} + \frac{1}{12} \end{aligned}\right\} \quad (61)$$

$$A_{12}^{*} = \frac{\Omega_{12}^{(2,2)*}}{\Omega_{12}^{(1,1)*}}, \quad (62)$$

$$B_{12}^{*} = \frac{5\Omega_{12}^{(1,2)*} - 4\Omega_{12}^{(1,3)*}}{\Omega_{12}^{(1,1)*}}. \quad (63)$$

The thermal conductivity associated with the transfer of energy due to the translational degrees of freedom of the particles is [2; 3]:

$$\lambda_{tr} = \lambda_1 \frac{1 + b_{1\lambda}x_2 + b_{2\lambda}x_2^2}{1 + a_{1\lambda}x_2 + a_{2\lambda}x_2^2}, \quad (64)$$

where λ_1 the thermal conductivity of the monoatomic vapor.

The thermal conductivity due to the contribution of the internal degrees of freedom of the particles is [2; 3]:

$$\lambda_{int} = \lambda_1 \frac{4\sqrt{3}}{25}A_{12}^{*}\frac{2C_{p,2} - 5R}{2R}\frac{x_2}{1 - \left(1 - \frac{D_{21}}{D_{22}}x_2\right)}, \quad (65)$$

$$\frac{D_{21}}{D_{22}} = \frac{\sqrt{6}}{2}\frac{A_{12}^{*}}{A_{22}^{*}}\frac{1}{\beta_{12}^{2}}, \quad (66)$$

The «reaction» component of the thermal conductivity is:

$$\lambda_r = \lambda_1 \frac{0{,}2771A_{12}^{*}}{B_{12}^{*}}\left(\frac{D_0(T)}{RT}\right)^2 \frac{x_2(1 - x_2)}{(1 + x_2)^2}, \quad (67)$$

Where

$$\left.\begin{aligned} a_{1\lambda} &= \frac{4\sqrt{3}}{3}\cdot\frac{1\text{-}V^{(3)}}{1\text{-}V^{(1)}}\beta_{12}^2 + 0{,}3\sqrt{6}\,\frac{A_{12}^*}{1+V^{(1)}}\beta_1^{-2} \\ a_{2\lambda} &= -(a_{1\lambda}+1) + \sqrt{2}\,\frac{1+V^{(2)}}{1+V^{(1)}}\beta_2^2 \\ b_{1\lambda} &= -2\frac{V^{(1)}\text{-}V^{(4)}}{1+V^{(1)}} + 0{,}3\sqrt{3}\,\frac{A_{12}^*}{1+V^{(1)}}\beta_{12}^{-2} \\ b_{2\lambda} &= -\left(b_{1\lambda}\text{-}\frac{V^{(1)}\text{-}V^{(2)}}{1+V^{(1)}}\right) \end{aligned}\right\}, \tag{68}$$

$$A_{22}^* = \frac{\Omega_2^{(2,2)*}}{\Omega_2^{(1,1)*}}, \tag{69}$$

When $A_{22}^* = 1{,}2$ and $B_{12}^* = 1{,}2$ we have:

$$\left.\begin{aligned} a_{1\lambda} &= 1{,}3359\beta_{12}^2 + 0{,}6262\beta_1^{-2}\text{-}2 \\ a_{2\lambda} &= -(a_{1\lambda}+1) + 0{,}9272\beta_2^2 \\ b_{1\lambda} &= 1{,}4936 + 0{,}4428\beta_{12}^{-2} + 0.6262\beta_1^{-2} \\ b_{2\lambda} &= -(b_{1\lambda}+0{,}3445) \end{aligned}\right\}, \tag{70}$$

Having laid out expressions (64) and (65) in a row on a small parameter x_2 Yargin V.S. received [2, 3, 24, 68]:

$$\lambda(x_2, T) = \lambda_1(T)\left\{1 + \sum_{n=1}^{m} B_n x_2^n + B_p\left(\frac{T_p}{T}\right)^2 \frac{x_2(1\text{-}x_2)}{(1+x_2)^2}\right\}, \tag{71}$$

where

$$B_p = 0{,}3335\beta_{12}^{-2}, \tag{72}$$

$$B_n = B_n^{(n)} + B_n^{(BH)}, \tag{73}$$

$$\left.\begin{aligned} B_1^{(\Pi)} &= -a_{1\lambda} + b_{1\lambda} \\ B_2^{(\Pi)} &= -a_{1\lambda}B_1^{(\Pi)}\text{-}a_{2\lambda}b_{2\lambda} \\ &\cdots\ \cdots\ \cdots\ \cdots \\ B_n^{(\Pi)} &= -a_{1\lambda}B_{n-1}^{(\Pi)} + a_{2\lambda}B_{n-2}^{(\Pi)}, n \geq 3 \\ B_1^{(BH)} &= 0{,}3325\beta_{12}^2\left(\frac{C_{p,2}}{R}\text{-}\frac{5}{2}\right) \\ &\cdots\ \cdots\ \cdots\ \cdots \\ B_n^{(BH)} &= B_1^{(BH)}(1\text{-}1{,}2248\beta_1^{-2})^{n-1} \end{aligned}\right\}, \tag{74}$$

$$T_P = \frac{D_0(T)}{R}. \quad (75)$$

Equations (70) – (75) show that the coefficients *B* of the series for x_2 the viscosity and thermal conductivity of the alkali metal vapors depend only on the absolute cross-sections of the «atom-atom» $\Omega_{11}^{(2,2)*}$ collisions and the relative cross-sections of the «atom-molecule» collisions β_{12}^2.

Thus, the theory we considered [2; 3; 24; 68] makes it possible to process and compare the results of the experimental studies of the viscosity and thermal conductivity of the alkali metal vapor. Excess relative viscosity and thermal conductivity can be given as functions of the molar fraction of the molecular component x_2, and the coefficients of the approximating polynomial are known as the functions of the collision cross sections. Approximating equations (36), (71) make it possible to carry out a reasonable extrapolation of the coefficients of the viscosity and thermal conductivity of the alkali metal vapor outside of the experimental studies, as well as to establish the relationship between the viscosity and thermal conductivity through the particle collisions. For a monoatomic pair of the alkali metals from (1.5) and (1.35) we have [2; 24].

$$\frac{\lambda_1(T)}{\eta_1(T)} = \frac{0{,}312 \cdot 10^5}{M}. \quad (76)$$

We compare our cross-sections of the particle collisions with the literature data on the viscosity and thermal conductivity of cesium and rubidium in the gas phase.

A large number of works performed by various methods have been devoted to the experimental study of the alkali metal vapor viscosity. Almost all of them are limited to a temperature of 1800 K. The viscosity of steam at high temperatures was studied in only two studies [6; 8]. The analysis of the results of studies of the viscosity and thermal conductivity of cesium and rubidium vapor was performed in [2; 3; 68]. Most alkali metals with increasing pressure are characterized by an increase in thermal conductivity and a decrease in viscosity. The data of different authors on these coefficients, as a rule, agree well with each other. And only cesium falls out of the general picture, for him the results of experimental studies on the viscosity of different authors differ in the sign of the pressure effect, and in the thermal conductivity – in the magnitude of this effect.

The work is devoted to the experimental study of the viscosity of the cesium vapor [2; 3; 14; 18; 19; 20; 21; 22; 23; 48; 65; 71; 72].

Henson R. M., Stratton T. E., Toodd J. [22] conducted a study of the viscosity of the cesium vapor by the method of a straight capillary at T = 600 ... 1000 K, the experimental data are described by the equation:

$$\eta = (2{,}5 \pm 0{,}5) \cdot 10^{-7} \left(\frac{T}{650}\right)^{0,7}, Pa \cdot s \quad (75)$$

According to the authors, the error is ± 20%, the obtained experimental values of the viscosity are not given. The method of the experiment and the design of the installation are not described.

Lee D.I., Bonilla S.F. [18; 19] measured the viscosity coefficient of cesium vapor in the temperature range of 950 ... 1280 K at pressures of 40 ... 500 kPa using the spiral viscometer method. Two series of experiments were conducted, more than 70 experimental points were obtained, which are presented in the graphical form. The dependence of the viscosity on pressure is ambiguous. At the temperatures below 1080 K the vapor viscosity decreases with increasing pressure, and at the high temperatures increases. The authors point to a large scatter of experimental data of about 20 %. The smallest deviation is characterized by the points obtained at the atmospheric pressure, for which the smoothed data are described by the equation:

$$\eta \cdot 10^{7} = -648{,}14 + 1511{,}52\left(\frac{T}{1000}\right) - 628{,}65\left(\frac{T}{1000}\right)^{2}, Pa \cdot s \quad (76)$$

In the experiments [18; 19], the pressure drop across the capillary was set using an intermediate inert gas and measured with a differential manometer. The investigated cesium vapor came from the evaporator into the capillary, and then condensed in the flow meter. The measured volume of the flowmeter was pre-calibrated according to the height of the working area.

The geometric factor of the capillary was determined after its installation on the set place on experiments with argon. The viscosity of the cesium vapor was calculated by the Poiseuille formula taking into account:

a) correction for the curvature of the capillary;

b) slip correction;

c) correction for thermal expansion of the capillary;

d) correction for energy losses at the input.

To reduce the correction for the curvature of the capillary experiments were performed at the pressure drops in the working area, ensuring compliance with the Dean criterion:

$$Re \cdot \sqrt{d/D} \leq 6, \tag{78}$$

where Re – is the Reynolds number,

d – is the inner diameter of the capillary,

D – is the average diameter of the spiral.

In the first series of experiments, a capillary made of *S* 304 steel with an inner diameter of 0,822 mm was used. The viscosity of the cesium vapor in the temperature range 950 ... 1210 K at the atmospheric pressure was studied. Since the installation did not provide a system for distilling the liquid alkali metal from the flowmeter into the evaporator, after each cycle of experiments, the metal was distilled from the flowmeter into the evaporator – through a capillary. The second series of experiments provided a system for the distilling condensate from the flow meter into the evaporator, which in general increased the service life of the installation. A capillary made of Haines-25 alloy was used. In this series of experiments, the main array of the experimental viscosity values was obtained. In the installation, as the authors point out, during the second series of experiments there was a microcrack, the capillary was subjected to corrosion.

Tippetsckirch H.V. [21] studied the viscosity of the cesium vapor at the temperatures of 1602-1622 K and a pressure of 3,95 mPa. 4 experimental points near the saturation line were obtained. In the experiments [21], the purified cesium was placed in a vessel made of tungsten-rhenium alloy. The inner diameter of the vessel is 6,755 ± 0,005 mm, the height of the working part is 13,032 ± 0,01 mm. The mass of the filled metal was determined by weighing the vessel before and after filling and was 0,0913 ± 0,005 g. Then the vessel was mounted on a suspension, heated and brought to a state of torsional vibrations. The vapor viscosity was determined by the magnitude of the decrement of the damping attenuation of the vessel with the cesium gas.

The pressure in the experiments [21] was determined by the elasticity curve, the errors of the experimental data according to the authors are 5 %.

In the group of thermophysics MAI under the leadership of the Professor Vargaftik N. B. the viscosity of the cesium vapor in the temperature range 900 ... 1200 K at pressures of 50 ... 250 kPa was studied by the method

of a straight capillary [2; 3; 20; 25; 23; 25]. The installation was a closed circulation circuit made of stainless steel. The investigated metal vapor from the evaporator through the steam heater entered the steam dehumidifier, took the temperature of the experiment and passed through the capillary. After leaving the capillary, the steam condensed in the refrigerator and flowed into a U-shaped flowmeter. The flowmeter temperature was kept constant by means of a liquid thermostat. Condensate flow was determined by the time of passage of the metal level between the two contact needles of the flow meter, which were at different heights. The pressure difference at the measuring section of the viscometer was set through the intermediate inert gas and was measured with an oil manometer. Capillary outlet pressure was measured with a mercury manometer. The installation provided the ability to control the geometric factor of the capillary during experiments without draining the metal from the measuring element. The calculation of the viscosity of the cesium vapor was performed according to the Poiseuille formula with the corrections for the gas compressibility, inlet pressure loss, molecular slip and thermal expansion of the capillary.

32 experimental points were obtained in the work, experiments were performed on isobars. As a result, the viscosity of the cesium vapor decreases with increasing pressure. The authors estimate the accuracy of the obtained data at 2,5 %. Processing the results [2; 14; 25] gives:

$$\left.\begin{array}{l} \eta_1 \cdot 10^7 = 258 + 0{,}220(\mathrm{T}\text{-}900), \mathrm{Pa} \cdot \mathrm{s} \\ \eta = \eta_1(1\text{-}1.65x_2 + 3x_2^2), \mathrm{Pa} \cdot \mathrm{s} \end{array}\right\} \qquad (79)$$

that corresponds β_{12}^2.

At the Moscow Aviation Institute under the direction of Professor Vargaftik N. B. the viscosity of the cesium vapor was studied by means of a viscous meter with an annular channel. 167 values of the vapor viscosity in the temperature range 900-1770 K at pressures of 12-135 kPa were obtained (Vargaftik N. B., Dzis V. G., Stepanenko I. S., Yargin V. S.) [59; 65; 69; 70; 71; 72; 74; 77].

According to [18; 19], the viscosity of the atomic component is 12-15 % lower than according to the results [24; 25]. The intersections of the collisions of atoms, calculated by [18; 19], increase with temperature, which indicates a qualitative illegality of the dependence $\eta(T)$.

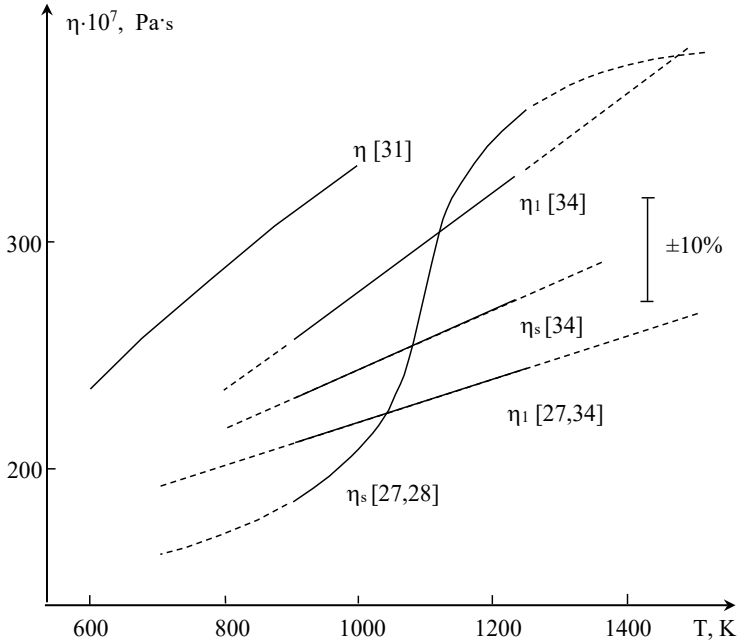

Figure 8. The viscosity of cesium in the gas phase according to the works [18; 19; 22; 23; 24; 25]

The negative effect of pressure [19] at T > 1050 K corresponds $\beta_{12}^2 \geq 2$, and its positive sign at T > 1080 K – $\beta_{12}^2 < 1{,}2$.

Rubidium. Two works have been devoted to the experimental study of the viscosity of rubidium in the gas phase [28; 34].

In [19] Bonilla C.F., Lee D.I. eliminating the shortcomings and methodological inaccuracies of the installation, diskovered during the experiments with the cesium vapor, conducted a study of the viscosity of the rubidium vapor in the temperature range of 930 ... 1230 K at pressures of 47 ... 200 kPa. The capillary of the viscometer was calibrated with argon before and after the experiments with the rubidium vapor. No changes in the geometric factor of the capillary during the experiments were detected. In [19], 49 experimental values of the viscosity of the rubidium vapor were obtained, which are shown graphically.

At a pressure of 100 kPa, the dependence of the viscosity on temperature, the authors [19] describe with the equation:

$$\eta \cdot 10^7 = -850{,}381 + 1644{,}192\frac{T}{1000} - 575{,}617\left(\frac{T}{1000}\right)^2, \; Pa \cdot s \qquad (80)$$

The negative effect of the pressure is established and the tables of the viscosity of the rubidium vapor in the temperature range 700-1500 K at pressures up to 500 kPa are developed. The dependence of the viscosity of a monoatomic pair on the temperature is described by the equation:

$$\eta_1 \cdot 10^7 = 241 + 0{,}300(T-1000), \; Pa \cdot s \qquad (81)$$

Processing of the experimental data of the work considered above in [5] gives:

$$\left.\begin{array}{c} \eta_1 \cdot 10^7 = 241 + 0{,}300(T-1000), \text{Па·с} \\ \Delta\eta = -2.08x_2 + 4{,}2x_2^2 - 8{,}4x_2^3 \\ \beta_{12}^2 = 2.4 \end{array}\right\}. \qquad (82)$$

M.I. Sidorov, Yu.V. Tarlakov, V.S. Yargin [25] conducted a study of the viscosity of the rubidium vapor by the viscometer with a straight line. 27 experimental values of the viscosity at T = 900 ... 1180 K and P = 40 ... 150 kPa were obtained, the authors estimate the accuracy of the obtained data at ± 2,5%.

The experiments [25] were performed on isobars 39, 76, 153 kPa. When processing the experimental data by extrapolation from the isotherms of the dependence at $x_2 \to 0$, the viscosity of the monoatomic pair was determined η_1 and the dependence was found, $\frac{(\eta_{эксп} - \eta_1)}{\eta_1}$, which was approximated by a second-order polynomial. The results of the processing give:

$$\left.\begin{array}{c} \eta_1 \cdot 10^7 = 239\text{-}0{,}210(T\text{-}900), \text{Па·с} \\ \eta = \eta_1(1\text{-}2.25x_2 + 5x_2^2) \end{array}\right\}. \qquad (83)$$

More accurate data processing [25] in [2; 3; 14] at the dissociation energy of the molecules D_0° = 48570 J/mol gives:

$$\left.\begin{array}{c} \eta_1 \cdot 10^7 = 259 - 0{,}202(T-1000), \text{Па·с} \\ \frac{\Delta\eta}{\eta_1} = -2.13x_2 + 4{,}4x_2^2 - 9x_2^3 \end{array}\right\}, \qquad (84)$$

that corresponds β_{12}^2 = 2,44.

Thus, in [19; 25] similar values of the cross sections of the «atom-molecule» collisions were obtained, and the values η_1 and their dependence on temperature differ slightly. The difference between η_1 in the above mentioned works does not exceed 9 % (Figure 9).

Later, the Moscow Aviation Institute conducted a study of the viscosity of the cesium vapor using a annular-type viscometer. 61 values of the viscosity of the rubidium vapor in the temperature range 990-1750 K at pressures of 39-135 kPa (Vargaftik N.B., Yargin V.S., Dzis V.G., Stepanenko I.S.) were obtained [66; 69; 72; 71; 77].

The viscosity and thermal conductivity of the alkali metal vapors are uniquely related through the cross sections of the collisions of the particles σ_{11}^2 and β_{12}^2. This allows us to jointly consider the experimental work with

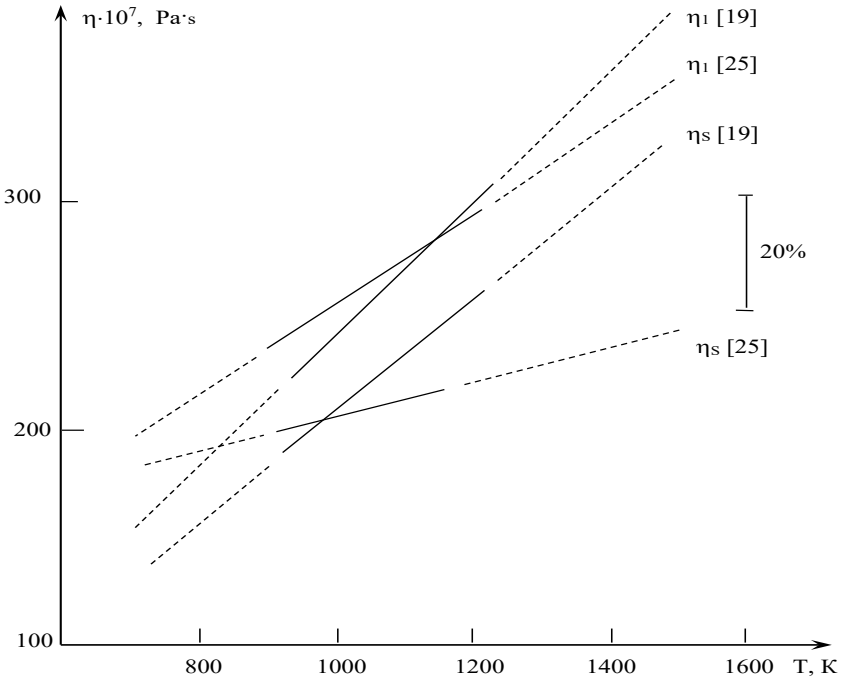

Figure 9. The viscosity of rubidium in the gas phase according to [19; 25]

these coefficients. Therefore lets consider the results of the experimental studies of the thermal conductivity, which can be used in the analysis of the viscosity data.

Information on experimental studies of the thermal conductivity of cesium in the gas phase are shown in the table 8.

Table 8

Experimental work on the thermal conductivity of cesium vapor

Authors	Lit. source	Interval		Method
		Temperature, K	Pressure, kPa	
Gottlieb M., Zollweg R.I.	[27]	950…1150	to 5.1	Combined method of flat layer and heated thread
Kitrilakis S., Meeker M.	[28]	1100…1400	to 67	Flat thermoionic converter
Martini W.R.	[29]	1240…1260	to 4	Flat thermoionic converter
Zarkova L.P., Stefanov B.I.	[12]	1000…2400	1…7	Modified method of heated thread
Zarkova L.P., Stefanov B.I.	[30]	600…1600	1…7	Modified method of heated thread
Lee D.I., Bonilla C.F	[31]	820…888	98…216	Periodic heating
Vargaftik N.B., Kerzhentsev V.V.	[32]	680…1080	10…130	Coaxial cylinders
Timroth D.L., Makhrov V.V., Sviridenko V.I., Reutov B.F.	[33]	800…1100	1.4…247	Heated thread with zero area
Vinogradov Yu.K., Veryugin A.V.	[13]	1120…1170	100…150	Periodic heating
Vinogradov Yu.K.	[34]	998…1707	12…195	Monotonous heating
Vinogradov Yu.K.	[39]	1000…1600	5…200	Monotone thermal mode method (automated version)

According to the results of [39], the dependence of the thermal conductivity of the cesium vapor on temperature is described by the equation:

$$\lambda_1 \cdot 10^4 = 15{,}2 + 59{,}7T, \mathrm{W/(m \cdot K)},$$

$$\beta_{12}^2 = 1{,}8.$$

The effect of pressure and magnitude β_{12}^2 can be judged by the data of works [13; 32; 34; 39], and the thermal conductivity of the atomic component by works [13; 32; 34; 39]. Dependencies λ_1(T) and λ_S(T) are shown in Figure 9.

The effective cross sections of the collisions of the atoms in works [22; 33; 34] are well coordinated with each other. The largest discrepancy in the cross sections is 5,5 %, i. e. is within the experimental errors. The data of the works [12; 30] differ by 10 ... 12% from the data [22; 33]. This discrepancy is explained by the fact that at the pressures of the experiments [12; 30] the free path length of atoms is close to the radius of the filament of the experimental installation and even exceeds it. Under such conditions, the Fourier heat equation needs to be clarified.

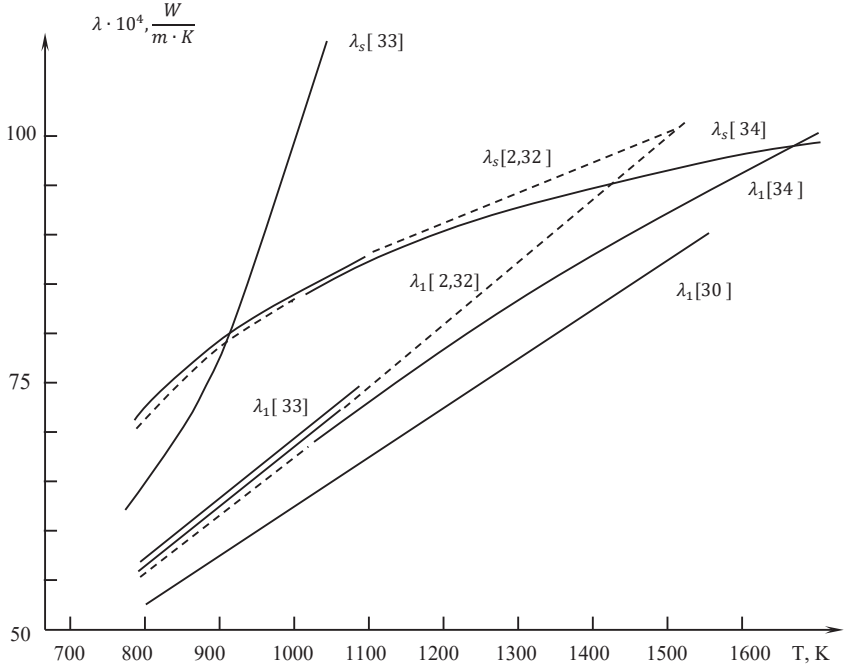

Figure 9. Thermal conductivity of cesium in the gas phase according to [2; 30; 32; 39; 33; 35; 34]

The value of the relative cross section β_{12}^2, determined by the effect of pressure according to [32], is 2,08, i. e. coincides within the errors with the results [34; 39]. The results [13] also confirm the data [32]. In [33] β_{12}^2 it obviously depends on the temperature and varies from 2,57 at T = 800 K to 0,96 at T = 1100 K.

Rubidium. Experimental work on the thermal conductivity of the rubidium vapor is shown in the table 9, the results are presented in Figure10.

Table 9

Experimental work on the thermal conductivity of the rubidium vapor

Authors	Lit. source	Interval		Error, %	Method
		Temperature, K	Pressure, kPa		
Gottlieb M., Zollweg R.I.	[27]	950…1150	to 2,9	30	Combined method of flat layer and heated thread
Lee D.I., Bonilla C.F.	[31]	1045…1099	84…89	6	Periodic heating
Vargaftik N.B., Studnikov E.L.	[36]	800…1110	5…150	4	Coaxial cylinders
Timroth D.L., Makhrov V.V., Reutov B.F.	[37]	900…1100	1.4…130	7	Heated thread with zero area
Vinogradov Yu.K.	[39]	970…1715	1,5…75	5-6	Monotone thermal mode method (automated version)

The first experimental works [27; 31] have methodological inaccuracies, which have been repeatedly discussed in the literature [2, 4]. The results of [36; 37; 39] with an accuracy of 2 ... 3% are consistent with each other, which is much less than the error of the experiments. The effective cross sections of the atoms $\sigma_{11}^2\Omega_{11}^{(2,2)*}$, the temperature dependence λ_1(T) and the value of the relative cross section «atom – molecule» β_{12}^2 according to the data of these works are close.

Analyzing experimental work on the thermal conductivity of cesium and rubidium in the gas phases, preference should be given to the work of Vinogradov Yu.K. [39]. The dependence of the thermal conductivity of the monoatomic vapor on temperature is described by the equation:

$$\lambda_1 \cdot 10^4 = 4{,}9 + 89{,}5T, W/(m \cdot K).$$

The relative cross sections of the «atom molecule» collisions depend on the temperature:

$$\text{e}\,\beta_{12}^2 = 2{,}24 - 0{,}1 \cdot \frac{T}{1000}.$$

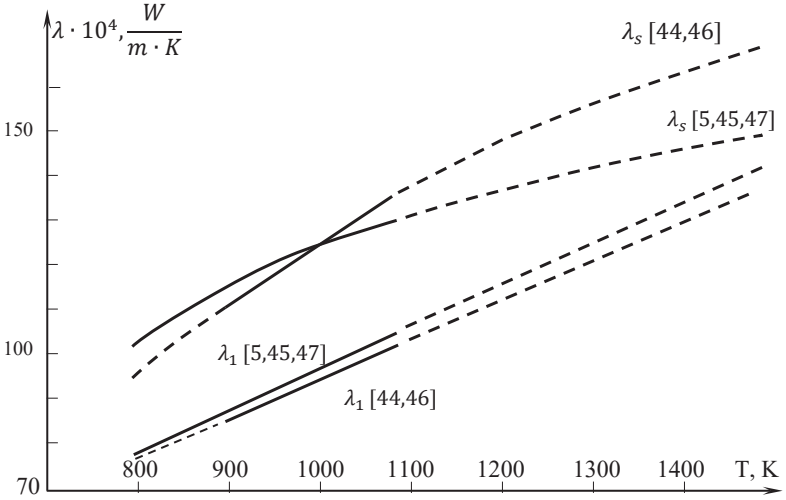

Figure 10. Thermal conductivity of rubidium in the gas phase according to [2; 36; 37]

We compare the obtained cross sections of the cesium and rubidium vapor microparticles with the literature data (Figure 11).

Figure 11 shows that the obtained cross sections of the «atom-atom» $\sigma_{11}^2\Omega_{11}^{(2,2)^*}$ collisions of our work for the Cs pair at T ≤ 1200 K almost coincide with the results [33] and agree well with the data of RSD 81 [68] tables and average cross-sectional values based on joint processing of the experimental viscosity and thermal conductivity data [2; 3]. With an accuracy of 4 ... 7 %, i. e. within the total error are consistent with the data [25]. At the temperatures up to 1300 K, the cross sections $\sigma_{11}^2\Omega_{11}^{(2,2)^*}$ agree within the total error with the data [34], but with increasing temperature they diverge, and at T = 1800 K the discrepancy is 13%. This discrepancy can be explained by the fact that at the temperatures above 1300 K for the cesium vapors

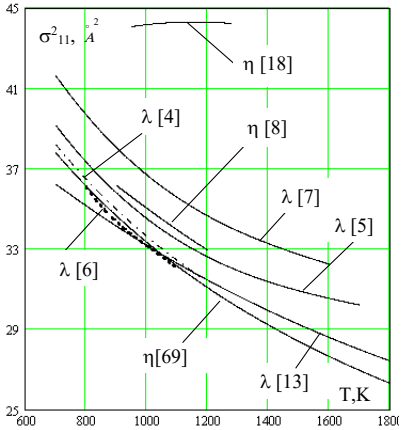

Figure 11. Effective collision cross sections atoms in the cesium pair

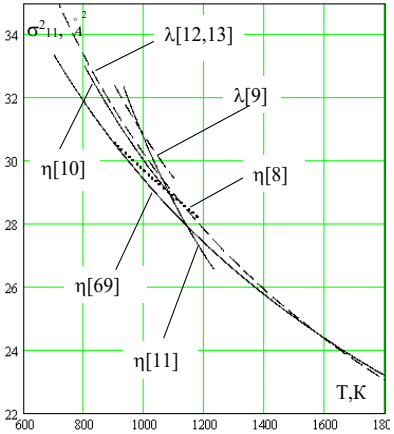

Figure 12. Effective sections of collisions rubidium pair atoms

$(\lambda_s - \lambda_1)/\lambda_1 \sim 5 \ldots 10\,\%$ [2], and in the field of the experimental parameters [34] $(\lambda_s - \lambda_1)/\lambda_1 \sim 1{,}0 \ldots 3{,}0\,\%$, with the total error of the experiment $\lambda \sim 6\%$ and a small array of the experimental values, it is impossible to obtain sufficiently accurate intersections of collisions $\sigma_{11}^2 \Omega_{11}^{(2,2)*}$.

In addition, as shown in the paragraph 1.4, at high temperatures in the experiments on the thermal conductivity, it is necessary to introduce many different corrections, taking into account a number of side effects, which reduces the accuracy of the final results. In general, the results [34] qualitatively correctly reflect the general patterns of the transfer processes in the cesium vapors.

The effective collision cross sections $\sigma_{11}^2 \Omega_{11}^{(2,2)*}$ for the *Rb* pair (Figure 12) according to the results of this work are consistent in the common areas of experiments at T ≤ 1200 K with the results of [18; 25; 39; 45] and differ from some of them in the field of extrapolation. Depending on the temperature of the collisions $\sigma_{11}^2 \Omega_{11}^{(2,2)*}$ for all works on the viscosity and thermal conductivity of the *Rb* vapor are different. This is due to the fact that they are all made in a narrow range of temperatures, which does not allow to reliably establish the temperature dependence $\sigma_{11}^2 \Omega_{11}^{(2,2)*}(T)$.

From the experiments on the viscosity of this work we can clearly ascertain a negative effect of the pressure for *Cs* and *Rb* ($\beta_{12}^2 > 1{,}21$). For all experimental points ($(\lambda - \lambda_1)/\lambda_1 \leq 0$), i. e. the viscosity decreases with the increasing pressure (increasing concentrations of the diatomic molecules x_2).

According to the relative intersections of the collisions β_{12}^2 in the pair *Cs* (Table 10), the data of this work are consistent with the data [25; 32; 34; 39]. Exceptions are works [18; 19; 33], at the temperature T ~ 1080 K there is a sharp change in β_{12}^2. The data from this work do not confirm this effect (see tables 10, 11).

The relative collisions of β_{12}^2 for the pair *Rb* according to the results of our work are consistent with the literature data obtained from the experimental data on the viscosity and thermal conductivity at $T = 700 \ldots 1200$ K (Table 12).

Table 10

Relative cross-sections of the β_{12}^2 cesium collisions in the gas phase based on the results of the viscosity and thermal conductivity works ($\Delta\beta_{12}^2 \sim 20\%$)

Source	[18, 19]	[25]	[32]	[33]	[34]	[39]	[69]
β_{12}^2	2,5-1,0	2,08	2,1	2,56-0,96	2,1	1,8	2,2

Table 11

Relative cross-sections of the β_{12}^2 cesium in the gas phase according to the results of the experimental viscosity research [69] ($\Delta\beta_{12}^2 \sim 30\%$)

T, K	914	975	1050	1135	1235	1330
Numeric points	10	15	23	21	23	14
β_{12}^2	2,4	1,9	2,3	2,1	2,6	1,9

Table 12

Relative cross-sections of the β_{12}^2 rubidium collisions in the gas phase based on the results of the viscosity and thermal conductivity works ($\Delta\beta_{12}^2 \sim 20\%$)

Source	[19]	[25]	[36]	[37]	[39]	[69]
β_{12}^2	2,44	2,4	2,21	2,17	$2{,}24 - 0{,}1\frac{T}{1000}$	2,3

Thus, the intersections of the collisions $\sigma_{11}^2\Omega_{11}^{(2,2)^*}$ and β_{12}^2 in the pair *Cs* and *Rb* for T ≤ 1200 K obtained in this work are in good agreement with most of the experimental works on the viscosity and thermal conductivity. The cross sections $\sigma_{11}^2\Omega_{11}^{(2,2)^*}$ were obtained by us from the processing of the viscosity experiments performed in a wider range of temperatures, which increases the reliability of the dependence $\sigma_{11}^2\Omega_{11}^{(2,2)^*}(T)$. These circumstances allow us to use the cross sections $\sigma_{11}^2\Omega_{11}^{(2,2)^*}$ and β_{12}^2 obtained in this paper to develop the recommended tables of coefficients of the viscosity and thermal conductivity of cesium and rubidium in the gas phase.

Cesium and rubidium have rather low ionization potentials, so various ionization processes can take place in their pair [10; 40; 41; 43]. Let us estimate the contribution of the electronic component λ_e to the thermal conductivity of steam and the ionic component to the viscosity.

In order of magnitude, the effect of the electronic component λ_e on the thermal conductivity is [42]:

$$\frac{\lambda_e}{\lambda_1} = \frac{N_e}{N_a}\frac{\sigma_{11}^2}{\sigma_{e1}^2}\sqrt{\frac{M}{m_t}}, \qquad (85)$$

where m_e – the mass of electrons, M – the mass of the atom, N_e and N_a – the concentration of electrons and atoms in the alkali metal vapor, σ_{e1}^2 and σ_{11}^2 the effective cross sections of the collisions «atom-electron» and «atom-atom». For rough estimates we accept $\sigma_{e1}^2 = \sigma_{11}^2$ and we receive (table 13).

Let's evaluate the viscosity of the weakly ionized alkali metal vapor [41; 42]:

$$\eta \sim \frac{\sqrt{T \cdot M}}{\sigma_{11}^2 + \sigma_p^2 \cdot \frac{N_i}{N_a}}, \qquad (86)$$

Table 13

Influence of electronic component on the vapor thermal conductivity *Cs* and *Rb*

T, K	Cesium		Rubidium	
	λ_e/λ_1, %		λ_e/λ_1, %	
	P = 1 kPa	P = 20 kPa	P = 1 kPa	P = 20 kPa
1500	0,8	0,5	0,2	0,15
1800	7,8	1,8	2,6	0,6
2000	40	33	16,9	12,0

where, σ_p^2 – the effective cross section of the resonant ion recharging on the neutral atom, N_i and N_a the concentration of ions and atoms in the pair.

At an ion energy 0,1-0,2 eB $\sigma_p^2 \sim 450 \div 500\ A^2$ [41; 42; 43], therefore, according to the equations (3, 21) the effect of the ionic component on the viscosity of cesium and rubidium vapor at low pressures is:

Table 14

Influence of the ionic component on the vapor viscosity

T, K	Cesium		Rubidium	
	η_e/η_1, %		η_e/η_1, %	
	$P = 0{,}1$ kPa	$P = 1$ kPa	$P = 0{,}1$ kPa	$P = 1$ kPa
1800	1	0,5	0,4	0,2
2000	6	2	3	0,9

Tables 13 and 14 show that at temperatures up to 2000 K and pressures $P \geq 10$ *кПа* the influence of the ionization processes on the transfer coefficients of the cesium and rubidium vapor can be neglected, and the vapor of these metals can be considered as a reactive two-component mixture of atoms and diatomic molecules.

Based on the parameters η_0, A, β_{12}^2 obtained in this work, according to the method [2; 3] of equation (19–42, 51–76) the tables of the viscosity and thermal conductivity of the rubidium and cesium vapor in the temperature range 700-2000 K at pressures 1-1500 kPa, including the saturation line were developed the vapor pressure at the saturation line was determined by [51], the vapor composition x_2 (molar concentration of two-volume molecules) by equation [2].

The coefficients of the thermal conductivity and viscosity of cesium vapor are in a good agreement with the data of [2; 3; 14; 32; 36; 39; 46] in their common temperature ranges, the maximum discrepancy does not exceed 5%. Within the total error, the tabular values of η_S and λ_S of our studies are consistent with [75], and η_1 and λ_1 for temperatures of 700… 1500 K. The maximum deviation is 12% at T > 180 K.

The tabular values of the coefficients of the thermal conductivity and viscosity of the rubidium vapor within the total errors are consistent with the data of [3; 5; 14; 25; 35; 37; 38; 39; 46], the maximum deviation does not exceed 6%.

Thus, the obtained in this paper tabular values of the coefficients of the viscosity of cesium and rubidium vapor in the gas phase, are quite consistent with the literature data for temperatures up to 1500 K.

The tables of the transfer coefficients developed by us are based on the experimental data on viscosity of the cesium and rubidium vapor the experiments have been carried out in a wide range of temperatures 900… 1750 K, which increases the reliability of extrapolation to high temperatures up to 2000 K. These circumstances recommend the developed viscosity and thermal conductivity tables for practical engineering calculations, and the values of the cross sections of absolute collisions «atom-atom» $\sigma_{11}^2\Omega_{11}^{(2,2)*}$ and relative collisions «atom-molecule» β_{12}^2 for research.

The calculated values of the coefficients of viscosity and thermal conductivity are given in the table 15 ... 25, Figures 13-16 (where η_1 and λ_1 – viscosity and thermal conductivity of the monoatomic vapor; η_S and λ_S – viscosity and thermal conductivity at the saturation line; λ_S' – components of thermal conductivity at the saturation line; λ_f – «frozen» component of thermal conductivity; λ_r – conductive component; x_2 – mole fraction of molecules; P_S – vapor pressure at the saturation line).

Table 15

Viscosity of cesium in the gas phase η · 10⁷, Pa · s

T, K	η_1	P, kPa									η_S
		1	10	25	50	100	400	600	1000	1500	
700	215,6	215,7									203,6
750	228,4	226,6	212,6								212,4
800	241,2	240,0	230,2								220,6
850	254,0	253,2	246,1	236,0							228,4
900	266,8	266,2	261,0	253,1	242,1						235,9
950	279,6	279,1	275,2	269,0	260,0	245,4					243,1
1000	292,4	292,0	288,9	284,1	276,7	264,1					250,2
1050	305,2	304,9	302,4	298,5	292,4	281,7					257,2
1100	318,0	317,8	315,8	312,5	307,4	298,3					264,1
1150	330,8	330,6	329,0	326,3	322,0	314,1	279,8				271,0
1200	343,6	343,4	342,0	339,8	336,1	329,3	298,1	283,5			277,9
1250	356,4	356,3	355,1	353,1	350,0	344,1	315,8	301,8			284,9
1300	369,2	369,1	368,1	366,4	363,7	358,4	332,8	319,6	299,2		291,9

(End of Table 15)

T, K	η_1	P, kPa									η_S
		1	10	25	50	100	400	600	1000	1500	
1350	382,0	381,9	381,0	379,5	377,2	372,6	349,3	336,9	317,2		299,0
1400	394,8	394,7	393,9	392,6	390,5	386,4	365,3	353,7	334,8	316,7	306,2
1450	407,6	407,5	406,8	405,7	403,8	400,1	380,9	370,1	352,0	334,3	313,6
1500	420,4	420,3	419,7	418,7	417,0	413,7	396,1	386,0	368,9	351,7	321,1
1550	433,2	433,1	432,6	431,7	430,1	427,2	411,0	401,6	385,3	368,7	328,6
1600	446,0	445,9	445,4	444,6	443,2	440,5	425,6	416,8	401,4	385,4	336,4
1650	458,8	468,7	458,3	457,5	456,3	453,8	440,1	431,8	417,3	401,8	344,2
1700	471,6	471,6	471,1	470,4	469,3	467,0	454,3	446,6	432,8	417,9	352,2
1750	484,4	484,4	484,0	483,3	482,3	480,2	468,4	461,2	448,1	433,8	360,3
1800	497,2	497,2	496,8	496,6	495,2	493,3	482,3	475,5	463,1	449,5	368,5
1850	510,0	510,0	509,6	509,1	508,2	506,4	496,1	489,7	478,0	464,9	376,7
1900	522,8	522,8	522,5	521,9	521,1	519,4	509,8	503,8	492,6	480,1	384,9
1950	535,6	536,6	535,3	534,8	534,0	532,4	523,4	517,7	507,1	495,1	–
2000	548,4	548,4	548,1	547,7	546,9	545,4	536,9	531,5	521,5	510,0	–

Table 16

Thermal conductivity of cesium in the gas phase $\lambda \cdot 10^4$, W/(m · K))

T, K	λ_1	P, kPa									λ_S
		1	10	25	50	100	400	600	1000	1500	
700	50,6	53,7									62,9
750	53,6	55,3	67,2								67,4
800	56,6	57,5	64,9								71,5
850	59,6	60,2	64,8	70,9							75,3
900	62,6	63,0	65,9	70,2	75,7						78,6
950	65,6	65,8	67,8	70,7	74,8	80,8					81,6
1000	68,6	68,8	70,1	72,2	75,1	79,8					84,4
1050	71,6	71,7	72,6	74,1	76,3	79,9					86,9
1100	74,6	74,7	75,3	76,4	78,0	80,8					89,2
1150	77,6	77,7	78,1	78,9	80,1	82,2	89,8				91,3
1200	80,6	80,6	81,0	81,6	82,5	84,1	90,3	92,6			93,4
1250	83,6	83,6	83,9	84,3	85,0	86,2	91,3	93,3			95,3
1300	56,6	56,6	86,8	87,1	87,7	88,6	92,7	94,5	96,6		97,2
1350	89,6	89,6	89,8	90,0	90,4	91,2	94,5	95,9	97,8		99,1
1400	92,6	92,6	92,7	92,9	93,2	93,8	96,5	97,7	99,3	100,4	100,9

(End of Table 16)

T, K	λ_1	P, kPa									λ_S
		1	10	25	50	100	400	600	1000	1500	
1450	95,6	95,6	96,7	95,8	96,1	96,5	98,6	99,6	101,0	102,0	102,7
1500	98,6	98,6	98,7	98,8	99,0	99,3	101,0	101,8	102,9	103,8	104,6
1550	101,6	101,6	101,7	101,7	101,9	102,2	103,5	104,1	105,1	105,7	106,5
1600	104,6	104,6	104,6	104,7	104,8	105,0	106,1	106,6	107,3	107,9	108,4
1650	107,6	107,6	107,6	107,7	107,8	107,9	108,7	109,1	109,7	110,1	110,4
1700	110,6	110,6	110,6	110,7	110,7	110,8	111,4	111,7	112,2	112,5	112,4
1750	113,6	113,6	113,6	113,6	113,7	113,8	114,2	114,4	114,7	114,9	114,3
1800	116,6	116,6	116,6	116,6	116,7	116,7	117,0	117,2	117,4	117,5	116,3
1850	119,6	119,6	119,6	119,6	119,6	119,7	119,9	120,0	120,1	120,1	118,7
1900	122,6	122,6	122,6	122,6	122,6	122,6	122,8	122,8	122,8	122,8	121,1
1950	125,6	125,6	125,6	125,6	125,6	125,6	125,7	125,7	125,6	125,6	–
2000	128,6	128,6	128,6	128,6	128,6	128,6	128,6	128,5	128,5	128,3	–

Table 17

The reaction component of the thermal conductivity *Cs* in the gas phase $\lambda_r \cdot 10^4$, W/(m · K)

T, K	λ_1	P, kPa									λ'_{P_S}
		1	10	25	50	100	400	600	1000	1500	
700	50,6	3,7	17,1								14,9
750	53,6	2,1	10,8								17,3
800	56,6	1,2	7,0								19,5
850	59,6	0,8	4,7	15,4							21,3
900	62,6	0,5	3,2	10,7	18,6						22,6
950	65,6	0,3	2,3	7,6	13,7	22,7					24,0
1000	68,6	0,2	1,7	5,5	10,2	17,6					25,0
1050	71,6	0,2	1,3	4,1	7,7	13,7					25,8
1100	74,6	0,1	1,0	3,1	5,9	10,8					26,4
1150	77,6	0,1	0,8	2,4	4,6	8,6	23,6				26,8
1200	80,6	0,1	0,6	1,9	3,7	6,9	20,1	25,4			27,1
1250	83,6	0,1	0,5	1,8	2,9	5,6	17,2	22,2			27,4
1300	86,6	0,1	0,4	1,2	2,4	4,6	14,7	19,3	25,6		27,6
1350	89,6	0,0	0,3	1,0	2,0	3,8	12,7	16,9	23,0		27,6
1400	92,6	0,0	0,3	0,8	1,7	3,2	10,9	14,8	20,6	26,3	27,7
1450	95,6	0,0	0,2	0,7	1,4	2,7	9,5	13,0	18,4	23,1	27,7

(End of Table 17)

T, K	λ_1	P, kPa									λ'_{P_S}
		1	10	25	50	100	400	600	1000	1500	
1500	98,6	0,0	0,2	0,6	1,2	2,4	8,3	11,5	16,5	21,1	27,6
1550	101,6	0,0	0,2	0,5	1,0	2,0	7,3	10,2	14,9	19,2	27,6
1600	104,6	0,0	0,2	0,5	0,9	1,8	6,4	9,0	13,4	17,6	27,5
1650	107,6	0,0	0,1	0,4	0,8	1,6	5,7	8,1	12,1	16,0	27,4
1700	110,6	0,0	0,1	0,3	0,7	1,4	5,1	7,2	10,9	14,6	27,3
1750	113,6	0,0	0,1	0,3	0,6	1,2	4,5	6,5	9,9	13,4	27,2
1800	116,6	0,0	0,1	0,3	0,5	1,1	4,1	5,8	9,0	12,3	27,1
1850	119,6	0,0	0,1	0,2	0,5	1,0	3,7	5,3	8,2	11,3	26,1
1900	122,6	0,0	0,1	0,2	0,4	0,9	3,3	4,8	7,5	10,4	26,0
1950	125,6	0,0	0,1	0,2	0,4	0,8	3,0	4,4	6,9	9,6	–
2000	128,6	0,0	0,1	0,2	0,4	0,7	2,7	4,0	6,3	8,8	–

Table 18

«Frozen» component of the thermal conductivity Cs in the gas phase $\lambda_f \cdot 10^4$, W/(m · K)

T, K	λ_1	P, kPa									λ'_{fS}
		1	10	25	50	100	400	600	1000	1500	
700	50,6	49,9									47,9
750	53,6	53,2	50,1								50,1
800	56,6	56,3	54,1								52,1
850	59,6	59,4	57,8	55,6							54,0
900	62,6	62,5	61,3	59,5	57,1						55,8
950	65,6	65,5	64,6	63,2	61,1	58,1					57,5
1000	68,6	68,5	67,8	66,7	65,0	62,2					59,4
1050	71,6	71,5	70,9	70,0	68,6	66,2					61,1
1100	74,6	74,5	74,1	73,3	72,1	70,0					62,8
1150	77,6	77,5	77,2	76,5	75,5	73,6	66,2				64,5
1200	80,6	80,5	80,2	79,7	78,8	77,2	70,2	67,2			66,2
1250	83,6	83,6	83,3	82,8	82,1	80,6	74,1	71,2			67,9
1300	86,6	86,6	86,3	85,9	85,3	84,0	78,0	75,1	71,0		69,7
1350	89,6	89,6	89,4	89,0	88,4	87,3	81,8	79,0	74,8		71,4
1400	92,6	92,6	92,4	92,1	91,6	90,6	85,5	82,9	78,7	75,1	73,2
1450	95,6	95,6	95,4	95,1	94,7	93,8	89,1	86,6	82,6	78,9	75,1
1500	98,6	98,6	98,4	98,2	97,8	97,0	92,7	90,3	86,4	82,7	77,0
1550	101,6	101,6	101,4	101,2	100,8	100,1	96,2	94,0	90,2	86,5	78,9

(End of Table 18)

T, K	λ_1	P, kPa									λ'_{fs}
		1	10	25	50	100	400	600	1000	1500	
1600	104,6	104,6	104,5	104,3	103,9	103,3	99,6	97,5	93,9	90,3	80,9
1650	107,6	107,6	107,5	107,3	107,0	106,4	103,0	101,1	97,6	94,1	83,0
1700	110,6	110,6	110,5	110,3	110,0	109,5	106,4	104,5	101,3	97,9	85,1
1750	113,6	113,6	113,5	113,3	113,1	112,6	109,7	107,9	104,8	101,5	87,1
1800	116,6	116,6	116,5	116,4	116,1	115,6	113,0	111,3	108,4	105,2	89,3
1850	119,6	119,6	119,5	119,4	119,2	118,7	116,2	114,7	111,9	108,8	91,8
1900	122,6	122,6	122,5	122,4	122,2	121,8	119,4	118,0	115,4	112,4	94,4
1950	125,6	125,6	125,5	125,4	125,2	124,8	122,6	121,3	118,8	116,0	–
2000	128,6	128,6	128,5	128,4	128,2	127,9	125,8	124,5	122,2	119,5	–

Table 19

Molar fraction of the diatomic vapor molecules *Cs* X_2,%

T, K	P, kPa									At saturation curve	
	1	10	25	50	100	400	600	1000	1500	X_2	P_s, kPa
700	0,775									3,33	4,524
750	0,456	4,22								4,29	10,15
800	0,286	2,72								5,31	20,59
850	0,130	1,82	4,33							6,36	36,34
900	0,163	1,27	3,06	5,78						7,43	66,56
950	0,093	0,92	2,23	4,27	7,91					8,50	$1,090 \cdot 10^2$
1000	0,069	0,68	1,66	3,22	6,07					9,56	$1,696 \cdot 10^2$
1050	0,052	0,52	1,27	2,48	4,74					10,58	$2,536 \cdot 10^2$
1100	0,040	0,40	0,99	1,95	3,75					11,57	$3,649 \cdot 10^2$
1150	0,032	0,32	0,79	1,56	3,02	10,33				12,51	$5,687 \cdot 10^2$
1200	0,026	0,26	0,64	1,26	2,46	8,65	12,03			13,40	$6,896 \cdot 10^2$
1250	0,021	0,21	0,52	1,04	2,04	7,29	10,25			14,23	$9,119 \cdot 10^2$
1300	0,018	0,18	0,44	0,87	1,70	6,20	8,79	13,26		15,01	$1,180 \cdot 10^3$
1350	0,015	0,15	0,37	0,73	1,44	5,31	7,59	11,58		15,73	$1,496 \cdot 10^3$
1400	0,013	0,13	0,31	0,62	1,23	4,68	6,59	10,16	13,97	16,39	$1,864 \cdot 10^3$
1450	0,011	0,11	0,27	0,53	1,06	3,98	5,75	8,95	12,42	16,99	$2,285 \cdot 10^3$
1500	0,009	0,09	0,23	0,46	0,92	3,48	5,05	7,92	11,08	17,54	$2,760 \cdot 10^3$
1550	0,008	0,08	0,20	0,40	0,80	3,07	4,47	7,05	9,93	18,04	$3,291 \cdot 10^3$
1600	0,007	0,07	0,18	0,36	0,71	2,71	3,97	6,30	8,92	18,47	$3,877 \cdot 10^3$
1650	0,006	0,06	0,16	0,32	0,63	2,42	3,54	5,68	8,04	18,87	$4,519 \cdot 10^3$

(End of Table 19)

T, K	P, kPa									At saturation curve	
	1	10	25	50	100	400	600	1000	1500	X_2	P_s, kPa
1700	0,006	0,06	0,14	0,28	0,56	2,16	3,18	5,09	7,28	19,21	$5{,}215 \cdot 10^3$
1750	0,005	0,05	0,13	0,25	0,50	1,94	2,86	4,60	6,61	19,52	$5{,}967 \cdot 10^3$
1800	0,005	0,05	0,11	0,23	0,48	1,78	2,59	4,17	6,02	19,80	$6{,}776 \cdot 10^3$
1850	0,004	0,04	0,10	0,20	0,41	1,69	2,36	3,80	5,50	20,06	$7{,}644 \cdot 10^3$
1900	0,004	0,04	0,09	0,19	0,37	1,45	2,14	3,47	5,04	20,31	$8{,}577 \cdot 10^3$
1950	0,003	0,03	0,08	0,17	0,34	1,32	1,96	3,19	4,64	–	–
2000	0,003	0,03	0,08	0,15	0,31	1,21	1,80	2,93	4,27	–	–

Table 20

Viscosity of rubidium in the gas phase $\eta \cdot 10^7$, Pa · s

T, K	η_1	P, kPa									η_S
		1	10	25	50	100	400	600	1000	1500	
700	198,5	194,2									186,2
750	210,1	207,6									193,7
800	221,8	220,2	207,4								200,8
850	233,4	232,4	223,4	211,1							207,4
900	245,1	244,3	237,9	228,5	215,8						213,9
950	256,7	256,2	251,4	244,2	233,8						220,1
1000	268,4	268,0	264,3	258,7	250,3	236,5					226,2
1050	280,0	279,7	276,9	272,4	265,6	253,8					232,2
1100	291,7	291,4	289,2	285,6	280,0	270,0					238,2
1150	303,3	303,1	301,3	298,4	293,7	283,3	249,8				244,2
1200	315,0	314,8	313,3	310,9	307,0	299,8	267,7	253,0			250,2
1250	326,6	326,5	325,3	323,2	319,9	313,7	284,8	270,8			256,3
1300	338,3	338,2	337,1	335,4	332,6	327,2	301,2	288,0	267,9		262,4
1350	349,9	349,8	348,9	347,4	345,0	340,4	317,0	304,6	285,3		268,6
1400	361,6	361,5	360,7	359,4	357,3	353,2	332,2	320,7	302,2	284,6	274,8
1450	373,2	373,2	372,5	371,3	369,5	365,9	346,9	336,3	318,7	301,5	281,1
1500	384,9	384,8	384,2	383,2	381,6	378,4	361,2	351,3	334,7	318,1	287,6
1550	396,5	396,5	395,9	395,1	393,6	390,7	375,1	366,0	350,3	334,3	294,1
1600	408,2	408,1	407,7	406,9	405,5	403,0	388,7	380,3	365,6	350,2	300,8
1650	419,8	419,8	419,4	418,6	417,5	415,1	402,1	394,3	380,4	365,7	307,5
1700	431,5	431,5	431,1	430,4	429,3	427,2	415,3	408,0	395,0	380,9	314,5

(End of Table 20)

T, K	η_1	P, kPa									η_S
		1	10	25	50	100	400	600	1000	1500	
1750	443,1	443,1	442,8	442,2	441,2	439,2	428,2	421,5	409,3	395,9	321,5
1800	454,8	454,8	454,4	453,9	453,0	451,2	441,0	434,8	423,3	410,5	328,7
1850	466,4	466,4	466,1	465,6	464,8	463,1	453,7	447,9	437,0	424,9	336,1
1900	478,1	478,1	477,8	477,3	476,6	475,0	466,3	460,8	450,6	439,1	343,7
1950	489,7	489,7	489,5	489,0	488,3	486,9	478,8	473,6	464,0	453,1	-
2000	501,4	501,4	501,1	500,7	500,1	498,8	491,1	486,3	477,2	466,8	-

Table 21

Thermal conductivity of Rb in the gas phase $\lambda \cdot 10^4$, W/(m · K)

T, K	λ_1	P, kPa									λ_S
		1	10	25	50	100	400	600	1000	1500	
700	72,4	79,9									93,4
750	76,7	80,5									100,2
800	80,9	83,0	98,8								106,4
850	85,1	86,4	96,1	108,4							111,9
900	89,4	90,1	96,3	104,7	115,2						116,7
950	93,6	94,1	98,1	103,9	111,7						121,0
1000	97,9	98,2	100,9	104,9	110,5	119,1					124,8
1050	102,1	102,4	104,2	107,0	111,1	117,7					128,3
1100	106,4	106,5	107,8	109,8	112,8	117,9					131,4
1150	110,6	110,8	111,6	113,1	115,3	119,1	132,6				134,3
1200	114,9	115,0	115,6	116,7	118,3	121,2	132,3	136,3			137,0
1250	119,1	119,2	119,7	120,4	121,7	123,9	132,9	136,5			139,5
1300	123,4	123,4	123,8	124,4	125,3	127,0	134,3	137,4	141,2		142,0
1350	127,6	127,7	127,9	128,4	129,1	130,4	136,3	139,0	142,4		144,7
1400	131,9	131,9	132,1	132,5	133,0	134,0	138,8	141,0	144,0	146,1	147,1
1450	136,1	136,2	136,3	136,6	137,0	137,8	141,5	143,3	145,8	147,7	149,2
1500	140,4	140,4	140,5	140,7	141,0	141,6	144,5	146,0	148,1	149,7	151,5
1550	144,6	144,7	144,7	144,9	145,1	145,6	147,9	149,0	150,7	152,1	153,8
1600	148,9	148,9	149,0	149,1	149,3	149,6	151,4	152,3	153,7	154,8	156,2
1650	153,1	153,2	153,2	153,3	153,4	153,7	155,1	155,8	156,9	157,8	158,7
1700	157,4	157,4	157,4	157,5	157,6	157,8	158,8	159,4	160,2	160,9	161,2
1750	161,6	161,7	161,7	161,7	161,8	161,9	162,7	163,1	163,7	164,2	163,7
1800	165,9	165,9	165,9	166,0	166,0	166,1	166,7	166,9	167,4	167,7	166,3

(End of Table 21)

T, K	λ_1	P, kPa									λ_s
		1	10	25	50	100	400	600	1000	1500	
1850	170,1	170,2	170,2	170,2	170,2	170,3	170,7	170,9	171,1	171,3	169,1
1900	174,4	174,4	174,4	174,4	174,4	174,5	174,7	174,8	175,0	175,0	171,9
1950	178,6	178,7	178,7	178,7	178,7	178,7	178,8	178,8	178,9	178,8	-
2000	182,9	182,9	182,9	182,9	182,9	182,9	182,9	182,9	182,8	182,7	-

Table 22

Reaction component of the steam thermal conductivity *Rb*

$\lambda_r \cdot 10^4$,W/(m · K)

T, K	λ_1	P, kPa									λ'_{rs}
		1	10	25	50	100	400	600	1000	1500	
700	72,4	9,1									25,3
750	76,7	4,8									29,3
800	80,9	2,7	23,0								32,6
850	85,1	1,6	14,6	31,1							35,7
900	89,4	1,0	9,5	21,3	36,0						38,1
950	93,6	0,7	6,4	14,8	26,2						40,0
1000	97,9	0,5	4,4	10,5	19,2	32,5					41,4
1050	102,1	0,3	3,2	7,6	14,2	25,0					42,5
1100	106,4	0,2	2,3	5,6	10,7	19,3					43,3
1150	110,6	0,2	1,8	4,3	8,2	15,1	40,6				43,9
1200	114,9	0,1	1,3	3,3	6,4	12,0	34,3	42,8			44,3
1250	119,1	0,1	1,1	2,6	5,0	9,6	29,0	37,1			44,5
1300	123,4	0,1	0,8	2,1	4,0	7,8	24,5	32,1	42,2		44,6
1350	127,6	0,1	0,7	1,7	3,3	6,4	20,9	27,9	37,6		44,9
1400	131,9	0,1	0,6	1,4	2,7	5,3	17,9	24,2	38,6	41,3	45,0
1450	136,1	0,0	0,5	1,1	2,3	4,4	15,3	20,9	29,7	37,2	44,7
1500	140,4	0,0	0,4	1,0	1,9	3,7	13,1	18,2	26,3	33,6	44,5
1550	144,6	0,0	0,3	0,8	1,6	3,2	11,4	15,9	23,4	30,3	44,3
1600	148,9	0,0	0,3	0,7	1,4	2,7	9,9	14,0	20,8	27,4	44,1
1650	153,1	0,0	0,2	0,6	1,2	2,4	8,7	12,4	18,6	24,6	44,0
1700	157,4	0,0	0,2	0,5	1,0	2,1	7,7	11,0	16,7	22,6	43,8
1750	161,6	0,0	0,2	0,5	0,9	1,8	6,8	9,8	15,0	20,4	43,6
1800	165,9	0,0	0,2	0,4	0,8	1,6	6,0	8,7	13,5	18,5	43,3
1850	170,1	0,0	0,1	0,4	0,7	1,4	5,4	7,8	12,2	16,9	43,1
1900	174,4	0,0	0,1	0,3	0,6	1,3	4,9	7,1	11,1	15,4	42,8
1950	178,6	0,0	0,1	0,3	0,6	1,1	4,4	6,4	10,1	14,1	-
2000	182,9	0,0	0,1	0,3	0,6	1,0	4,0	5,8	9,2	12,9	-

Table 23

«Frozen» component of the steam thermal conductivity of *Rb*

$\lambda_f \cdot 10^4$,W/(m · K)

T, K	λ_1	P, kPa									λ'_{3S}
		1	10	25	50	100	400	600	1000	1500	
700	72,4	70,9									68,1
750	76,7	75,7									70,9
800	80,9	80,3	75,8								73,6
850	85,1	84,8	81,5	77,3							76,1
900	89,4	89,1	86,8	83,6	79,2						78,6
950	93,6	93,4	91,7	89,1	85,5						81,0
1000	97,9	97,7	96,4	94,4	91,4	86,7					83,4
1050	102,1	102,0	101,0	99,3	96,9	92,7					85,7
1100	106,4	105,3	105,5	104,1	102,1	98,5					88,1
1150	110,6	110,6	109,9	108,8	107,1	104,0	92,0				90,4
1200	114,9	114,8	114,3	113,4	111,9	109,3	98,1	93,5			92,7
1250	119,1	119,1	118,6	117,9	116,6	114,3	104,0	99,4			95,0
1300	123,4	123,4	123,0	122,3	121,2	119,2	109,8	105,3	98,9		97,4
1350	127,6	127,6	127,3	126,7	125,8	124,0	115,4	111,1	104,5		99,7
1400	131,9	131,9	131,6	131,1	130,3	128,7	120,9	116,8	110,4	104,9	102,1
1450	136,1	136,1	135,9	135,4	134,7	133,3	126,2	122,3	116,1	110,5	104,6
1500	140,4	140,4	140,1	139,8	139,1	137,9	131,4	127,8	121,8	116,1	107,0
1550	144,6	144,6	144,4	144,1	143,6	142,4	136,5	133,1	127,4	121,8	109,5
1600	148,9	148,9	148,7	148,4	147,9	146,9	141,5	138,3	132,9	127,4	112,1
1650	153,1	153,1	153,0	152,7	152,2	151,3	146,3	143,4	136,3	132,9	114,7
1700	157,4	157,4	157,2	157,0	156,6	155,7	151,2	148,4	143,5	138,4	117,4
1750	161,6	161,6	161,5	161,3	160,9	160,1	155,9	153,4	148,8	143,6	120,2
1800	165,9	165,9	165,8	165,5	165,2	164,5	160,6	158,2	153,9	149,2	123,1
1850	170,1	170,1	170,0	169,8	169,5	168,9	165,3	163,0	158,9	154,4	126,0
1900	174,4	174,4	174,3	174,1	173,8	173,2	169,9	167,8	163,9	159,6	129,1
1950	178,6	178,6	178,5	178,4	178,1	177,6	174,4	172,5	168,5	164,7	-
2000	182,9	182,9	182,8	182,6	182,4	181,9	179,0	177,1	173,7	169,8	-

Table 24

Molar fraction of the diatomic vapor molecules of *Rb* X_2,%

T, K	P, kPa									At saturation curve	
	1	10	25	50	100	400	600	1000	1500	X_2	P_s, kPa
700	1,153									3,44	3,132
750	0,646									4,42	7,399
800	0,387	3,62								5,46	16,66
850	0,245	2,35	5,51							6,53	30,27
900	0,163	1,59	3,79	7,07						7,60	54,31
950	0,113	1,11	2,69	5,11						8,66	91,63
1000	0,081	0,80	1,95	3,76	7,03					9,70	$1{,}463\cdot10^2$
1050	0,060	0,59	1,46	2,83	5,38					10,70	$2{,}235\cdot10^2$
1100	0,045	0,45	1,11	2,18	4,18					11,67	$3{,}284\cdot10^2$
1150	0,035	0,35	0,87	1,70	3,30	11,14				12,58	$4{,}666\cdot10^2$
1200	0,028	0,28	0,69	1,36	2,64	9,20	12,74			13,45	$6{,}436\cdot10^2$
1250	0,022	0,22	0,55	1,10	2,15	7,65	10,73			14,26	$8{,}651\cdot10^2$
1300	0,018	0,18	0,45	0,90	1,77	6,42	9,08	13,65		15,03	$1{,}137\cdot10^3$
1350	0,015	0,15	0,38	0,75	1,47	5,42	7,74	11,79		15,74	$1{,}463\cdot10^3$
1400	0,013	0,13	0,32	0,63	1,24	4,62	6,64	10,23	14,06	16,40	$1{,}849\cdot10^3$
1450	0,011	0,11	0,27	0,53	1,05	3,96	5,73	8,91	12,37	17,01	$2{,}298\cdot10^3$
1500	0,009	0,09	0,23	0,45	0,90	3,43	4,97	7,80	10,93	17,56	$2{,}816\cdot10^3$
1550	0,008	0,08	0,20	0,39	0,78	2,98	4,36	6,87	9,69	18,08	$3{,}400\cdot10^3$
1600	0,007	0,07	0,17	0,34	0,68	2,61	3,82	6,07	8,62	18,54	$4{,}057\cdot10^3$
1650	0,006	0,06	0,15	0,30	0,60	2,30	3,38	5,40	7,70	18,95	$4784\cdot10^3$
1700	0,005	0,05	0,13	0,26	0,53	2,04	3,00	4,82	6,91	19,31	$5{,}562\cdot10^3$
1750	0,005	0,05	0,12	0,23	0,47	1,82	2,68	4,32	6,22	19,63	$6{,}448\cdot10^3$
1800	0,004	0,04	0,10	0,21	0,42	1,63	2,40	3,88	5,62	19,90	$7{,}360\cdot10^3$
1850	0,004	0,04	0,09	0,19	0,37	1,46	2,16	3,61	5,09	20,12	$8{,}372\cdot10^3$
1900	0,003	0,03	0,08	0,17	0,34	1,32	1,96	3,18	4,63	20,29	$9{,}420\cdot10^3$
1950	0,003	0,03	0,08	0,15	0,30	1,20	1,78	2,89	4,22	20,42	0,1051E+05
2000	0,003	0,03	0,07	0,14	0,28	1,09	1,62	2,64	3,86	20,50	0,1165E+05

The errors of the tabular values of the coefficients of the viscosity and thermal conductivity are (estimation of errors was carried out according to the method [56; 57]):

for cesium:

at $T \le 1600\,K,\ \eta_l = 3\%,\ \eta_s = 5\%,\ \lambda_l = 4\%,\ \lambda_s = 6\%;$

at $T \le 1750\,K,\ \eta_l = 4{,}5\%,\ \eta_s = 7\%,\ \lambda_l = 5\%,\ \lambda_s = 8\%;$

at $T > 1750\,K,\ \eta_l = 5\%,\ \eta_s = 10\%,\ \lambda_l = 8\%,\ \lambda_s = 10\%;$

for rubidium:

at $T \le 1600\,K,\ \eta_l = 3{,}5\%,\ \eta_s = 5\%,\ \lambda_l = 4{,}5\%,\ \lambda_s = 6\%;$

at $T \le 1750\,K,\ \eta_l = 5\%,\ \eta_s = 7\%,\ \lambda_l = 5{,}5\%,\ \lambda_s = 8\%;$

at $T > 1750\,K,\ \eta_l = 6\%,\ \eta_s = 10\%,\ \lambda_l = 7\%,\ \lambda_s = 10\%.$

In practice, the coefficients of the thermal conductivity and viscosity of the alkali metals in the gas phase can be conveniently calculated by the ratios [2]:

$$\eta(T, x_2) = \eta_l(T)\left(1 + \sum_{n=1}^{m} A_n x_2^n\right), \qquad (87)$$

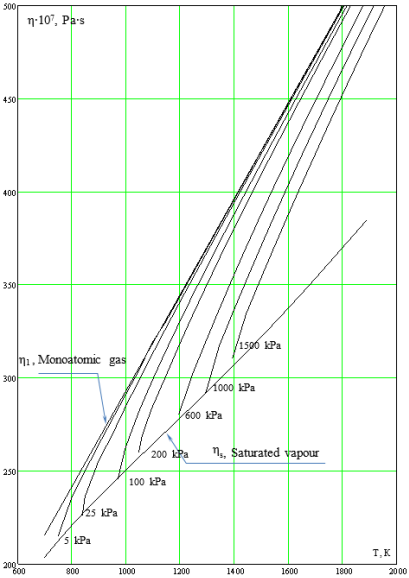

Figure 13. Viscosity of the cesium vapor

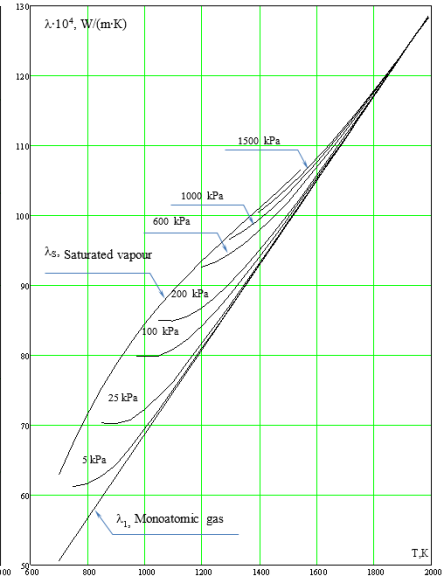

Figure 14. Thermal conductivity of the cesium vapor

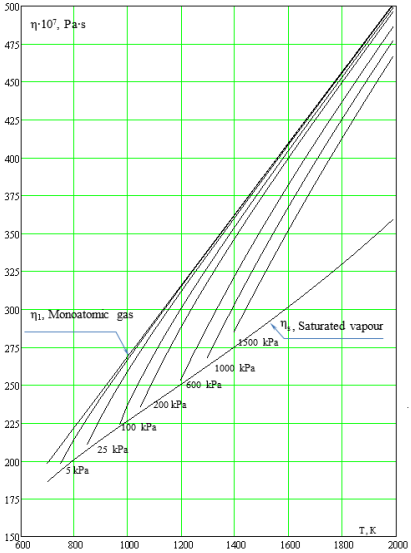

Figure 15. Viscosity of rubidium vapor

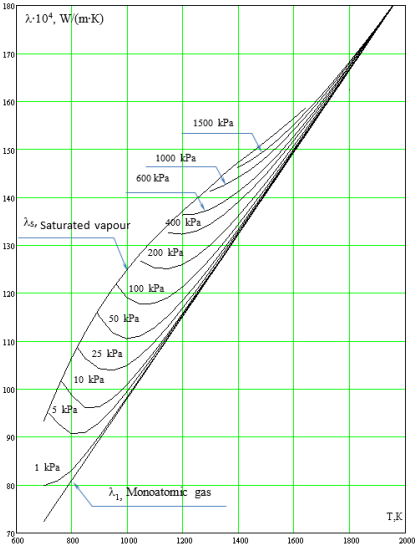

Figure 16. Thermal conductivity of the rubidium vapor

$$\lambda(T,x_2)=\lambda_1(T)\left(1+\sum_{n=1}^{m}(B_n^{BH}+B_n^{\Pi})x_2^n+B_p(\Delta H/RT)^2x_2(1-x_2)/(1+x_2)^2\right) \quad (88)$$

$$\lambda_{BH}(x_2,T)=\lambda_1(T)\sum_{n=1}^{m}B_n{}^{BH}x_2^n\,, \quad (89)$$

$$\lambda_{\Pi}(x_2,T)=\lambda_1(T)(1+\sum_{n=1}^{m}B_n{}^{\Pi}x_2^n)\,, \quad (90)$$

$$\lambda_{з}(x_2,T)=\lambda_1(T)(1+\sum_{n=1}^{m}B_nx_2^n)\,, \quad (91)$$

$$\lambda_{з}(x_2,T)=\lambda_1(T)(1+\sum_{n=1}^{m}B_nx_2^n)\,, \quad (92)$$

$$\lambda_p(x_2,T)=B_p\left(\frac{T_p}{T}\right)^2\frac{x_2(1-x_2)}{(1+x_2)^2}\,, \quad (93)$$

where x_2 – is the molar fraction of the diatomic molecules in the alkali metal vapor, ΔH – the thermal effect of the dissociation reaction of molecules at temperature T, coefficients: $A_n, B_n^{BH}.B_n^{\Pi}, B_p$ are given in the table, they are determined by the relative collisions and thermodynamic constants of the alkali metal vapor, their numerical values are given in the table 25.

Table 25

Coefficients of equations (87-93)

n	1	2	3	1	2	3
Coefficient	**Rubidium**			**Cesium**		
A_n	-1.916	3.594	-6.615	-1.762	3.073	-5.256
B_n	-2.172	4.171	-7.903	-1.987	3.571	-6.316
B_n^n	-2.374	4.414	-8.195	-2.231	3.852	-6.640
B_n^{BH}	0.202	-0.243	0.292	0.244	-0.281	0.324
B_P	0.145	0.151				

The coefficients of the viscosity and thermal conductivity of cesium and rubidium in the gas phase on isobars are quite accurately approximated by polynomials of the third degree:

$$\eta \cdot 10^7 = \sum_0^3 c_n \tau^n, \quad \Pi a \cdot c, \tag{94}$$

$$\lambda \cdot 10^4 = \sum_0^3 b_n \tau^n, \quad \frac{Bm}{M \cdot K}, \tag{95}$$

where $\tau = \frac{T}{1000}$, $T = T^* ... 2000K$.

The approximation error is less than 1%, which is much lower than the errors of the tabular values η and λ. The coefficients of equations (94, 95) are given in table 26.

Tables 18 and 23 show that the «frozen» component of the thermal conductivity λ_3 for cesium and rubidium vapor decreases with increasing concentration of molecules, and the «reaction» λ_p component increases (Tables 17, 22). Their total contribution depends on the magnitude β_{12}^2 and values the of thermodynamic constants. For steam *Cs* and *Rb* the maximum value, the pressure effect for thermal conductivity $(\lambda_S - \lambda_1)/\lambda_1 \approx 10 \div 30\%$

acquires at $T = 700...1300K$ (Tables 16, 21, Figures 14, 16, 17), so outside the specified temperature range, determining the relative cross sections of collisions β_{12}^2 from the experimental data on the thermal conductivity is associated with significant difficulties. The viscosity depending on the pressure (concentration of molecules) for the alkali metal vapor varies significantly over a wide range of temperatures. For $T = 800...2000K$ the effect of pressure for the vapor viscosity *Cs* and *Rb* is $(\eta_l - \eta_S)/\eta_S \approx 10 \div 40\%$, therefore, in determining β_{12}^2 the preference should be given to the experimental data on the vapor viscosity of the alkali metals.

Table 26

Coefficients of equations (94, 95)

P, kPa	T*, K	a_0	a_1	a_2	a_3	b_0	b_1	b_2	b_3
1	2	3	4	5	6	7	8	9	10
		Viscosity				Thermal conductivity			
Rubidium									
25	850	-157.5	593.6	-225.1	46.5	260.5	-401.6	314.5	-66.7
50	900	-233.6	717.1	-293.2	59.2	324.5	-508.5	373.4	-77.4
100	1000	-298.9	800.2	-327.5	63.5	325.7	-477.8	336.9	-66.9
200	1050	-380.6	891.4	-358.7	51.2	387.2	-562.5	374.2	-72.1
400	1150	-444.2	928.7	-353.2	61.4	421.0	-591.2	376.8	-70.4
1000	1300	-508.6	923.7	-317.7	51.2	442.7	-582.5	350.8	-62.9
Ps	700	64.0	223.8	-85.5	23.8	-60.9	337.1	-195.0	43.2
Cesium									
25	850	-114.7	536.5	-174.5	36.0	123.0	-163.7	143.9	-30.7
50	900	-180.0	641.3	-232.3	45.7	157.0	-219.5	174.1	-35.8
100	1000	-247.4	730.9	-271.6	52.2	193.0	-274.4	201.6	-40.3
200	1050	-341.2	861.4	-337.0	54.2	198.5	-264.1	185.1	-35.3
400	1150	-522.1	1139.9	-494.5	95.1	175.7	-198.1	133.5	-23.2
1000	1300	-257.6	501.8	-56.3	0.04	304.9	-417.7	260.5	-47.9
P_s	700	59.7	264.9	-103.1	28.4	-49.8	248.8	-149.2	34.5

6. Conclusions

The monograph is devoted to the experimental study of the viscosity of cesium and rubidium in the gas phase in unexplored regions of high temperatures, as well as the development of calculation equations and tables of transfer coefficients of these substances at temperatures up to 2000 K.

Main results of the work:

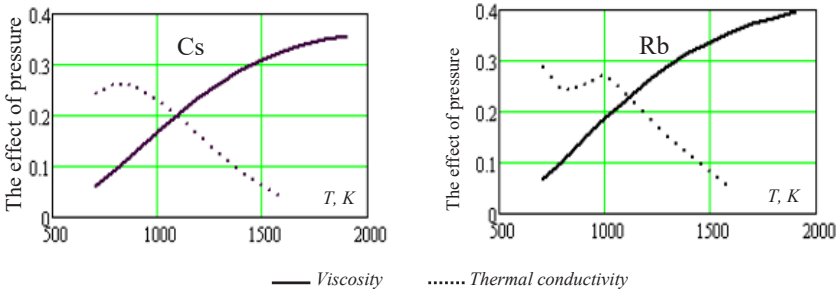

Figure 17. The effect of pressure in the pair of cesium and rubidium

An experimental installation for the study of the viscosity of the alkali metal vapor in a wide range of high (up to 2000 K) temperatures, implementing the method of a viscometer with an annular channel.

Have been developed high-temperature measuring cell, the design of which allows you to directly measure the temperature of the working element of the viscometer. This provides an accurate determination of the temperature of the investigated alkali metal vapor in the working gap.

The original method of stabilization of the steam generator operation mode was applied, which allowed to ensure the stationary flow of the investigated alkali metal vapor in the working element of the viscometer. Distinctive features of the created installation are high stability of modes of its work and considerable resource.

A large array of experimental data on the viscosity of the cesium vapor (167 points) and the rubidium vapor (61 points) at the following values of state parameters:

for cesium T = 900 ... 1770 K, P = 12 ... 135 kPa;

for rubidium T = 990 ... 1750 K, P = 39 ... 135 kPa.

Most of the obtained experimental data do not lie in the previously studied temperature range above 1200 K. The average error of the experimental data is 3%.

On the basis of the received experimental data dependences of the viscosity of steam of cesium and rubidium on temperature and structure (pressure) are established. The cross-sections of the «atom-atom» collisions and the relative cross-sections of the «atom-molecule» collisions are calculated.

Equations and tables of the viscosity and thermal conductivity of cesium and rubidium in the gas phase at T = 700 ... 2000 K and P = 1 ... 1500 kPa, including the saturation line were calculated. Obtained on the basis of experimental data [59; 61; 62; 65; 66; 69; 71; 72; 73; 74; 77; 80] on the viscosity of the rubidium and cesium vapor, the cross sections of the collisions agree well with the literature data, have high reliability and accuracy, so developed on their basis calculation equations and tables for the viscosity and thermal conductivity can be recommended for practical use in the scientific and engineering calculations by specialists in the field of research of properties of metals in the gas phase, creation of new types of the heat carriers and development of high-temperature power and technological equipment.

References:

1. Hirschfelder J., Curtiss C., Byrd R. (1961) *Molekulyarnaya teoriya gazov i zhidkostey* [Molecular theory of gases and liquids] / trans. with English. Moscow: Foreign. lit., 929 p.

2. Vargaftik N.B., Yarqin V.S. (1985) Theimat conductivity and viscosity of the gaseous phase. Handbook of Thermodynamic and Transport Ptopeities of Akali Metals. Ed, R. Ohse. Oxford: Btachwett Scientific Publications, pp. 785–842.

3. Yargin B.C. (1982) *Issledovanie protsessov perenosa v dissotsiirovannykh parakh shchelochnykh metallov* [Investigation of transfer processes in dissociated alkali metal vapors]: Dis. Dr. Tech. Sciences (specialty 01.04.14). Moscow: MAI, 288 p.

4. Shpilrain E.E., Yakimovich K.A., Totsky E.E. (1970) *Teplofizicheskie svoystva shchelochnykh metallov* [Thermophysical properties of alkali metals] / under ed. V.A. Kirillina. Moscow: Standartov Publishing House, 488 p.

5. Stepanenko I.F. etc. (1987) Ustanovka dlya izmereniya vyazkosti parov shchelochnykh metallov pri vysokikh temperaturakh [Installation for measuring the viscosity of alkali metal vapors at high temperatures]. *Measuring equipment*. no. 8, pp. 62–65.

6. Stepanenko I.F. (1988) *Eksperimental'noe issledovanie i razrabotka tablits vyazkosti litiya i natriya v gazovoy faze* [Experimental study and development of lithium and sodium viscosity tables in the gas phase]: Diss. Cand. those. Science. Moscow: MAI, 127 p.

7. Bystrov P.I., Kagan D.N., Krechetov G.A., Spielrein E.E. (1988) *Zhidkometallicheskie teplonositeli teplovykh trub i energeticheskikh ustanovok* [Liquid metal heat carriers of heat pipes and power plants]. Moscow: Nauka, 263 p.

8. Dolgov V.I. (1983) *Eksperimental'noe i teoreticheskoe issledovanie vyazkosti litiya v gazovoy faze* [Experimental and theoretical study of lithium viscosity in the gas phase]: Dis. Cand. physical mat. Science. Moscow: MAI, 250 p.

9. Greensburg B.I. (1986) *Sozdanie i issledovanie rubidiy-gelievogo i kaliy-gelievogo kvantovykh magnitrometrov* [Development and research of rubidium-helium and potassium-helium quantum magnetrometers]: Abstract dis. Cand. physical and mathematical Science. Leningrad, 18 p.

10. Klyucharev A.I., Janson M.L. (1988*) Elementarnye protsessy v plazme shchelochnykh metallov* [Elementary processes in plasma of alkali metals]. Moscow: Energoatomizdat, 224 p.

11. Vargaftik N.B., Voljak L.D. (1985) Thermodynamic Properties of Alkali Metal Vapours at Low Pressures. Handbook of Thermodynamic and Transport Properties of Alkali Metals. Ed. R. Ohse. Oxfotd: Black-well Scientific Publications, pp. 535–576.

12. Zarkova L.P., Stefanov B.I. (1965) Eksperimental'noe opredelenie koeffitsienta teploprovodnosti tsezievoy plazm [Experimental determination of the thermal conductivity of cesium plasmas]. *International. symp. on properties and application of low-temperature plasma at XX International. congr. in theoretical and applied chemistry. Collection of reports*. Moscow, pp. 239–247.

13. Vinogradov Yu.K., Veryugin A.Z. (1978) Eksperimental'noe issledovanie teploprovodnosti metodom periodicheskogo nagreva [Experimental study of thermal conductivity by periodic heating]. *Engineering Physics Journal*, no. 5, vol. 34. pp. 854–859.

14. Yargin B.C., Sidorov N.I., Studnikov E.L. (1978) *Vyazkost' i teploprovodnost' shchelochnykh metallov v gazovoy faze. Obzory po teplofizicheskim svoystvam veshchestv* [Viscosity and thermal conductivity of alkali metals in the gas phase. Reviews on the thermophysical properties of substances]. TFTS: IVTAN, 131 p.

15. Yargin B.C. (1975) Osobennosti protsessov perenosa v parakh shchelochnykh metallov [Features of transfer processes in alkali metal vapors]. *Sat. Thermophysical properties of working fluids and coolants of new technology*. Moscow: MAI, pp. 75–90.

16. Hirschfeldeir J.O. (1957) Heat Conductivity in Polyatomic or Etectronicallu Excited Cases. II. J. Chem. Phys., vol. 26, no. 2, pp. 282–285.

17. Stefanov B. (1980) Generalization of thermal conductivity and viscosity data for monatomic alkali metal vapours. High Temperatures-High Pressures, vol. 12, pp. 189–194.

18. Lee D.I., Bonilla C.F. Viscosity of the Atkali Metal Vapours. Part 1. Cesium up to 5 bars and 1000 °C. Alkali Metals Int. Symposium. Nottingam. 1966, Spec. Pub., no. 22, 1967, pp. 53–74.

19. Lee D.I., Bonilla C.F. (1968) The viscosity of the Alkali Metal Vapors. Nucl End. and Design, no. 5, pp. 455–469.

20. Vargaftik N.B., Sidorov N.I., Tarlakov Yu.V. (1972) Eksperimental'noe issledovanie vyazkosti parov tseziya [Experimental study of the viscosity of cesium vapor]. *Thermophysics of high temperatures*, vol. 10, no. 6, pp. I203–I2C9.

Tippetsckirch H.V. (1976) Viscosities of Cesium Vapor to 1620 K and Liquid Gallium to 1800 K. Berichte der Bunsengcsellschaft fur Physikalische Chemie, B. 80, no. 8.

21. Henson R. M., Stratton T. E., Toodd J. (1964) Viscosity of CesiumVapor. Bull. Am. Phys. Soc. 3er 2. V. 9. P. 156.

22. Sidorov N.I. (1972) Eksperimentalnoe issledovanie vyazkosti parov tseziya: Diss. kand. tehn. nauk. Moscow: MAI, 166 p.

23. Yargin V.S. (1978) Osobennosti teploprovodnosti schelochnyih metallov v gazovoy faze. Svyaz mezhdu teploprovodnostyu i vyazkostyu. *Inzhenerno-fizicheskiy zhurnal*, t. 34, no. 3, pp. 456–465.

24. Sidorov N.I., Tarlakov Yu.V., Yargin B.C. (1975) Rezultatyi eksperimentalnogo issledovaniya vyazkosti parov rubidiya i tseziya. *Izvestiya vuzov. Ser. Energetika*. Moscow, pp. 96–101.

25. Grosse A.V. (1968) High-Temperature Properties of Cesium. Inorganic Huctear Chemical Letters, V. 4, pp. 261–265.

26. Gottlieb M., Zollweg R.I. (1963) Thermal Conductivity of Cesium Vapor. In: Advanced Energy Conversion. Pergamon Press, V. 3, pp. 37–48.

27. Kitrilakis S., Meeker M. Experimental Determination of the Heat Conduction of Cesium Gas. I bid. P. 59–68.

28. Martini W.R. Theoretical Calculation of the Thermal Conductivity of Cesium Vapor at Thermoionic Temperatures. I bid. P. 49–58.

29. Zarkova L.P., Stefanov B.I. (1976) Izmerenie koeffitsienta teploprovodnosti gazov i parov do 2500 K. Pary rtuti i tseziya [Measuring the thermal conductivity of gases and vapors up to 2500 K. Vapors of mercury and cesium]. *Thermophysics of high temperatures*, vol. 14, no. 2, pp. 277–284.

30. Lee C.S., Bonilla C.F. (1967) Thermal Conductivity of the Atkati Metat Vapors and Arqon. Proc. of the 7th Conference on Thermal Conductivity. NBS, USA, pp. 561–578.

31. Vargaftik N.B., Kerzhentsev V.V. (1973) Eksperimental'noe issledovanie koeffitsienta teploprovodnosti para tseziya [Experimental study of the thermal conductivity of cesium vapor]. *Thermophysics of high temperatures*, vol. 10, no. 1, pp. 59–65.

32. Timrot D.L., Makhrov Z.V., Sviridenko.V.I., Reutov B.F. (1976) Eksperimental'noe issledovanie teploprovodnosti parov tseziya. [Experimental study of the thermal conductivity of cesium vapor]. *Thermophysics of high temperatures*, vol. 14, no. 1, pp. 67–74.

33. Vinogradov Yu.K. (1982) *Eksperimental'noe izuchenie temperaturnoy zavisimosti teploprovodnosti parov tseziya* [Experimental study of the temperature dependence of the thermal conductivity of cesium vapor], Moscow: MAI, 16 p. Dep. in VINITI, no. 5064-82.

34. Makhrov V.V. (1984) Razrabotka metodov issledovaniya, izmereniya teploprovodnosti perspektivnykh gazovykh teplonositeley s uchetom ikh akkomodatsii na tverdoy poverkhnosti i sostavlenie tablits transportnykh svoystv [Development of research methods, measurement of thermal conductivity of promising gas coolants, taking into account their accommodation on a solid surface and compilation of tables of transport properties]: Dis. Dr. tech. Sciences, Moscow: MPEI, 462 p.

35. Vargaftik N.B., Studnikov E.L. (1972) *Eksperimental'noe issledovanie teploprovodnosti parov rubidiya* [Experimental study of the thermal conductivity of rubidium vapor]. *Thermal power engineering*, pp. 81–83.

36. Timrot D.L., Makhrov V.V., Reutov B.F. (1978) *Eksperimental'noe issledovanie teploprovodnosti parov rubidiya* [Experimental study of the thermal conductivity of rubidium vapor]. *Thermophysics of high temperatures*, vol. 16, no. 5, pp. 943–945.

37. Studnikov E.L. (1972) *Eksperimental'noe issledovanie teploprovodnosti parov rubidiya* [Experimental study of the thermal conductivity of rubidium vapor]: Diss. cand. those. Sciences. Moscow, 166 p.

38. Vinogradov Yu.K. (1990) *Razrabotka nestatsionarnykh metodov issledovaniya teploprovodnosti gazov i izmerenie teploprovodnosti perspektivnykh gazovykh teplonositeley* [Development of non-stationary methods for studying the thermal conductivity of gases and measuring the thermal conductivity of promising gas coolants]. Abstract of diss. dr. tech. Sciences (specialty 01.04.14). Moscow: MPEI, 34 p.

39. Radtsig A.A., Smirnov B.M. (1986) *Parametry atomov i atomnykh ionov: Spravochnik. 2-e izd.* [Parameters of atoms and atomic ions: a Handbook. 2nd ed.]. Moscow: Energoatomizdat, 344 p.

40. Arefiev K.M. (1983) *Yavleniya perenosa v gaze i plazme* [Transport phenomena in gas and plasma]. Moscow: Energoatomizdat, 112 p.

41. Eletsky A.V., Palkina L.A., Smirnov B.M. (1975) *Yavlenie perenosa v slaboionizirovannoy plazme* [Transport phenomenon in weakly ionized plasma]. Moscow: Atomizdat, 333 p.

42. Galitsky Z.M., Nikitin E.E., Smirnov B.M. (1981) *Teoriya stolknoveniy atomnykh chastits* [Theory of collisions of atomic particles]. Moscow: Nauka, 256 p.

43. Gurvich L.V., Veits I.V., Medvedev V.A. et al. (1982) *Termodinamicheskie svoystva individual'nykh veshchestv: Spravochnoe izdanie: v 4-kh t.* [Thermodynamic properties of individual substances: Reference book: in 4 volumes], 3rd ed. revised and expanded. v. 4, book 1. Moscow: Nauka, 623 p.

44. Vargaftik N.B. (1972) *Spravochnik po teplofizicheskim svoystvam gazov i zhidkostey. Izd. 2-e, dop. i pererab* [Reference book on thermophysical properties of gases and liquids]. Ed. 2nd, add. and reworked. Moscow: Nauka, 720 p.

45. Vargaftik N.B., Filippov L.P., Tarzimanov A.A., Totsky E.E. (1990) *Spravochnik po teploprovodnosti zhidkostey i gazov* [Handbook of thermal conductivity of liquids and gases]. Moscow: Energoatomizdat, 352 p.

46. Borzhievsky A.A. (1986) *Issledovanie elektroprovodnosti neideal'noy tsezievoy plazmy na podogrevaemoy adiabaticheskoy trube* [Investigation of the

electrical conductivity of a nonideal cesium plasma in a heated adiabatic tube]. Diss. cand. Phys.-Math. Sciences. Dolgoprudny: MIPT, 156 p.

47. Timrot D.L. (1985) Issledovanie teploprovodnosti i vyazkosti parov shchelochnykh metallov na kafedre inzhenernoy teplofiziki MEI [Investigation of thermal conductivity and viscosity of alkali metal vapors at the Department of Engineering Thermal Physics of MPEI]. *Thermophysical properties of working fluids, coolants and structural materials of modern energy. Interuniversity thematic collection no. 72*. Moscow: MPEI, pp. 3–17.

48. Stefanov B.I., Timrot D.L., Totsky E.E., Zhu Wen-hao (1966) Eksperimental'noe issledovanie vyazkosti i teploprovodnosti parov natriya i kaliya [Experimental study of the viscosity and thermal conductivity of sodium and potassium vapors]. *Thermophysics of high temperatures*, vol. 4, no. 1, pp. 141–142.

49. Makarov V.E. (1987) *Eksperimental'noe issledovanie vyazkosti i teploprovodnosti parov natriya i kaliya* [Experimental research and development of viscosity tables for potassium steam]: Abstract of the thesis. diss. cand. tech. Sciences (specialty 01.04.14). Moscow: MAI, 18 p.

50. Mozgovoy A.G., Roshchupkin V.V., Pokrasin M.A. etc. (1988) *Litiy, natriy, kaliy, rubidiy, tseziy. Davlenie nasyshchennykh parov pri vysokikh temperaturakh* [Lithium, sodium, potassium, rubidium, cesium. Saturated vapor pressure at high temperatures]. USSR State Committee for Standards. Moscow: Publishing House of Standards, 38 p.

51. Idelchik I.E. (1975) *Spravochnik po gidravlicheskim soprotivleniyam* [Handbook of hydraulic resistance]. Moscow: Mashinostroenie, 559 p.

52. Aleshko P.I. (1977) *Mekhanika zhidkosti i gaza* [Mechanics of liquid and gas]. Kharkov: Vishcha shkola, 320 p.

53. Dinamicheskaya vyazkost' i teploprovodnost' geliya, neona, argona, kriptona i ksenona pri atmosfernom davlenii v intervale temperatur ot normal'nykh tochek kipeniya do 2500 K. GSSSD 17-81 [Dynamic viscosity and thermal conductivity of helium, neon, argon, krypton and xenon at atmospheric pressure in the temperature range from normal boiling points to 2500 K. GSSSD 17-81] / USSR State Committee for Standards. Moscow: Publishing house. standards, 1982.

54. Taylor J. (1985) *Vvedenie v teoriyu oshibok* [Introduction to the theory of errors] / per. from English. Moscow: Mir, 272 p.

55. Selivanov M.N., Fridman A.E., Kudryashova Zh.F. (1987) *Kachestvo izmereniy. Metrologicheskaya spravochnaya kniga* [Measurement quality. Metrological reference book]. Leningrad: Lenizdat, 295 p.

56. Ryabinovich S.G. (1978) *Pogreshnosti izmereniy* [Measurement errors]. Leningrad: Energy, 261 p.

57. Kucheruk I.M., Andrianov V.M. (1981) *Obrobka rezul'tativ fizichnikh doslidzhen'* [Obrobka results in physical studies]. Kiev: Vishcha shkola, 216 p.

58. Dzis V.G., Stepanenko I.F., Yargin B.C. (1989) *Eksperimental'noe issledovanie vyazkosti i razrabotka tablits koeffitsientov perenosa tseziya v gazovoy faze. MAI* [Experimental study of viscosity and development of tables of cesium transfer coefficients in the gas phase. MAI]. Moscow, 23 p. Dep. in VINITI 29.03.89, no. 2275-B89.

59. Lukin V.I., Ivakin B.A., Sustin P.E. (1981) Eksperimental'noe issledovanie vyazkosti i razrabotka tablits koeffitsientov perenosa tseziya v gazovoy faze. MAI [Viscosity of some gases, measured by the unsteady flow method]. *Journal of Technical Physics*, vol. 51, no. 4, pp. 860–862.

60. Dzis V.G., Dyachinska O.M. (2020) V'yazkist' ta teploprovidnist' pari luzhnikh metaliv. Rubidiy. Tseziy [Viscosity and thermal conductivity of the steam of puddle metals. Rubid. Cesium]. *Sciences of Europe*, vol. 1, no. 51, pp. 16–29.

61. Dzis V.G., Nikolyuk P.K., Dyachinska O.M., Bubnovska I.A. (2007) V'yazkist' pari tseziyu pri visokikh temperaturakh [Viscosity of cesium vapor at high temperatures]. Actual Problems of Scientific Research – 2007: materials of the III – International Scientific and Practical Conference, volume 7. Dnepropetrovsk: Science and Education, pp. 49–51.

62. Shpil'rain E.E., Yakimovich K.A. e.a. (1985) Density and Thermal Expansion of Liquid Alkali Metals. *Handbook of Thermodynamic and Transp ort Properties of Alkali Metals*. Ed. R. Ohse. Oxford: Blackwell Scientific Publications, pp. 435–469.

63. GOST 3044-84 *Preobrazovateli termoelektricheskie. Nominal'nye statich-eskie kharakteristiki preobrazovaniya* (1987) [Thermoelectric converters. Nominal static conversion characteristics]. Moscow: Publishing House of Standards, 78 p.

64. Dzis V.G., Stepanenko I.F., Sidorov N.I. and others (1988) *Eksperimental'noe issledovanie vyazkosti para tseziya pri temperaturakh 900-1250 K i davleniyakh 12-130 kPa* [Experimental study of the viscosity of cesium vapor at temperatures of 900-1250 K and pressures of 12-130 kPa]. Moscow: MAI, 12 p. Dep. in VINITI 26.03.88, no. 7576 – B88.

65. Dzis V.G., Stepanenko I.F., Yargin Z.S. (1989*) Rezul'taty eksperimen-tal'nogo issledovaniya vyazkosti rubidiya v gazovoy faze pri vysokikh temperaturakh* [Results of an experimental study of the viscosity of rubidium in the gas phase at high temperatures]. Moscow; MAI, 7 p. Dep. in VINITI 28.12.83, no. 215 – B89.

66. Gill F., Murray W., Wright M. (1985) *Prakticheskaya optimizatsiya* / per. s angl [Practical optimization / translated from English]. Moscow: Mir, 509 p.

67. Vargaftik N.B., Yargin B.C., Sidorov N.I. and etc. (1984*) Koeffitsienty dina-micheskoy vyazkosti i teploprovodnosti v gazovoy faze* [Alkali metals. Coefficients of dynamic viscosity and thermal conductivity in the gas phase], GSSSD R72-84. Moscow: GSSSD, 56 p.

68. Dzis V.G. (1990) *Ekperimental'noe issledovanie vyazkosti i razrabotka tablits koeffitsientov perenossa tseziya i rubidiya v gazovoy faze* [Experimental study of viscosity and development of tables of transfer coefficients of cesium and rubidium in the gas phase]. Diss. cand. tech. Sciences (specialty 01.04.14). Moscow: MAI, 136 p.

69. Dzis V.G., Stepanenko I.F., Yargin V.S. (1989) Rezul'taty eksperimen-tal'nogo issledovaniya vyazkosti para tseziya metodom viskozimetra s kol'tsevym kanalom [Results of an experimental study of the viscosity of cesium vapor by the method of a viscometer with an annular channel]. *Collection of scientific papers MPEI No. 204 "Issues of industrial technologies. Moscow energy institute*. Moscow, pp. 27–29.

70. Vinogradov Yu.K., Dzis V.G., Stepanenko I.F., Yargin V.S., Yakimovich Yu.K. (1989) Eksperimental'noe issledovanie protsessov perenosa shchelochnykh metallov v gazovoy faze pri temperaturakh 1200-2000 [Experimental study of transfer processes of alkali metals in the gas phase at temperatures of 1200-2000K]. *Thermophysical properties of substances. Proceedings of the VIII All-Union Conference. part 2*, Novosibirsk, pp. 144–148.

71. Dzis V.G., Stepanenko I.F., Yargin V.S. (1990) *Eksperimental'noe issledovanie vyazkosti i razrabotka tablits koeffitsientov perenosa tseziya i rubidiya v gazovoy faze pri vysokikh temperaturakh* [Experimental study of viscosity and development of tables of transfer coefficients for cesium and rubidium in the gas phase at high temperatures]. Dep. hands in VINITI No. 4206-90 dated 25.07.90.

72. Dzis V.G. (2020) Vyazkist i teploprovidnist pari tseziyu pri visokikh temperaturakh [Viscosity and thermal conductivity of cesium vapor at high temperatures]. *Slovak international scientific journal,* vol. 1, no. 40, pp. 31–34.

73. Vargaftik N.B., Vinogradov Yu.K., Dolgov V.I., Dzis V.G. and others (in all 7 authors) (1991) [Viscosity and thermal conductivity of alkali metals vapors at tem-peratures up to 2000 K]. *International Journal of Thermopphysics*, vol. 12, no. 1, pp. 85–103.

74. Vinogradov Yu.K., Sidorov N.I., Yargin V.S. (1984) Teploprovodnost' i vyazkost' parov tseziya [Thermal conductivity and viscosity of cesium vapors]. *Engineering Physics Journal*, vol. 46, no. 5, pp. 863–875.

75. Vinogradov Yu. K. (1992) Rubidium dissociated vapour heat conductivity at temperatures up to 2000 K. *Teplofizika vysokikh temperature*, vol. 30, no. 1, pp. 63–68.

76. Dzis V.G. (1990) Jeksperimental'noe issledovanie vjazkosti i razrabotka tablic kojefficientov perenosa cezija i rubidija v gazovoj faze [Experimental study of viscosity and development of tables for the transfer coefficients of cesium and rubidium in the gas phase]. Abstract dis. cand. tech. Sciences. Moscow: MAI, 20 p.

77. Dzis V.G., Stasenko V.A., Nikolyuk P.K., Shnyorko V.M. (2002) V'yazkist' ta teplo providnist' tseziyu ta rubidiyu v gazoviy fazi pri visokikh temperaturakh [Viscosity and thermal conductivity of cesium and rubidium in the gas phase at high emperatures]. *Scientific notes of Vinnytsia State Pedagogical University named after M. Kotsyubynsky.* Vinnytsia: VSPU, Issue 1: Physics and Mathematics, pp. 466–473.

78. Dzis V.G., Nikolyuk P.K., Bubnovska I.A., Dyachinska O.M. (2006) Koefitsiєnti perenosu pari rubidiyu [Rubidium bet transfer coefficient]. Conference «Actual Problems of Modern Sciences: Theory and Practice-2006» materials of the 3rd International Scientific and Practical. Dnipropetrovsk: Science and Education, vol. 22, pp. 49–52.

79. Dzis V.G., Dyachinska O.M. (2020) Eksperimental'ne doslidzhennya vyazkosti tseziyu i rubidiyu v gazoviy fazi [Experimental studies of the viscosity of cesium and rubidium in the gas phase]. *Danish Scientific Journal*, vol. 2, no. 37, pp. 37–51.